MASTER IN MOLECULAR MICROBIOLOGY

K+-dependent cell cycle regulation in Caulobacter crescentus

Collignon, Madeline

Award date:
2021

Awarding institution:
University of Namur

Faculty of Sciences

K^+-dependent cell cycle regulation in *Caulobacter crescentus*

Thesis conducted for obtaining
the academic degree of master 120 in molecular microbiology

Madeline Collignon
January 2021

University of Namur
FACULTY OF SCIENCES
Biology Department
Rue de Bruxelles 61-5000 NAMUR
Email: secretariat.bio@unamur.be

K^+-dependent cell cycle regulation in *Caulobacter crescentus*

Collignon Madeline

Abstract

Potassium (K^+) is the most abundant cation in all living cells. Besides its neutralizing and osmoprotective functions, this ion is crucial to the activity of the ribosomes and many intracellular enzymes. K^+ is also an important regulator of bacterial physiology as it is involved in diverse processes including biofilm formation, chemotaxis, cell to cell communication or virulence. Yet the role of K^+ in the bacterial cell cycle remains uncharacterized. By using flow cytometry, we have demonstrated in this work that K^+ is essential for cell cycle progression in *Caulobacter crescentus*. This α-proteobacterium possesses a putative K^+ channel and two K^+-uptake systems, Kup and Kdp. Presumably involved in K^+ uptake in low K^+ conditions, we have investigated the role of the Kdp transporter and the one of the KdpD/E two-component signal transduction system that regulates *kdp* expression. Deletion of the Kdp system impaired growth exclusively in low K^+, suggesting that as in *E. coli*, Kdp is mainly active in K^+ limiting conditions. In contrast, the KdpD/E two-component system seems to function in a different fashion. Both deletion and catalytic inactivation of the sensor kinase KdpD resulted in a growth surpassing the wild-type strain in low K^+ conditions. We found that the *kdp* operon was expressed even without KdpD activation, thus arguing for an alternative phosphodonor for its cognate response regulator KdpE. Our data also suggest that Kdp is likely involved in the K^+-dependent cell cycle progression. Overall, our work highlights the unsuspected and central role of K^+ in bacterial cell cycle regulation.

Thesis conducted for obtaining the academic degree of master 120 in molecular microbiology

Director of the thesis: Régis Hallez

Supervisor: Alex Quintero-Yanes

“Imagination is more important than knowledge.”

Albert Einstein

Acknowledgements

First of all, I would like to thank Alex for his trust in me with this project. Thank you for teaching and mentoring me during this year, but also for letting me fly on my own as your words were, I have certainly learned a lot from it. I wish you great achievements in the pursuit of your career and much happiness in your growing family. Thanks also to you, Régis for your guidance and good advice during this project.

I can't thank my team enough for welcoming me as one of their own: Aish, Aurélie, Tania, Anthony, Aravind, Elie, Jérôme and José. Any one of them would answer my questions and help me with great pleasure at any time (except perhaps Anthony but that's because I don't like pâté nor andouillettes). The great diversity of cultures, languages, and level of expertise in this team makes all its richness. Special thank you to my bench neighbour, Jérôme, who is always in a good mood and whose jokes are definitely not appreciated as much as they should be. Thanks also to you Aish, for being so encouraging and supportive, I wish you all the best in the continuation of your PhD in Namur.

Of course, this year would not have been the same without my MMM friends, Elisabeth, Hala, Max without forgetting The Fabulous Charline. We have spent together memorable moments in our beloved office whose walls will forever smell fries. Sharing our happy news, laughing at our stupid mistakes, crying over PCR, forbidding the words “writing” and “master thesis” in the same sentence, and lots of gossiping to keep us entertained. I’ll also remember our summer rosé afterworks and our pool parties in Ciney Beach (the place to be) between lockdowns. I hope that we will have the opportunity to get together in Germany and that we will keep in touch later on to hear all about your undoubtedly successful scientific careers.

Thank you to my family for supporting my moods and my doubts during these five years of studies. Thank you to my brother and my moms, for always believing in my abilities even when I did not. Thank you to my sisters Zoé and Jane, you are both the sunshine of my day and your innocence as children has many times brought me back to the essentials. I am grateful to have such a loving and caring family to come back to after short or long days of work.

Thanks to Valérie Charles and Kévin Willemart for their technical assistance with the ICP-OES and FACS equipment respectively. Thanks to Aurélie for purifying KdpE and teaching me the process of this purification. Thanks also to Pauline for welcoming me to her team for a day of fractionation training.

Lastly, I want to thank the members of my jury: Agnès Roba, Dr. François Beaufay and Prof. Jean-Yves Matroule for their time dedicated to this work.

Table of contents

Abbreviations

(p)ppGpp	guanosine tetra- and penta- phosphate
ADP	adenosine diphosphate
ATP	adenosine triphosphate
CA	catalytic ATP-binding
Ca^{2+}	calcium
c-di-AMP	c-di-adenosine monophosphate
c-di-GMP	c-di-guanosine monophosphate
ChIP-seq	chromatin immunoprecipitation followed by deep sequencing
Cs^{+}	cesium
DBD	DNA-binding domain
DHp	Dimerization Histidine phosphotransfer
DNA	Deoxyribonucleic acid
DRaCALA	differential radial capillary action ligand assays
EI	Enzyme I
EII	Enzyme II
FACS	Fluorescence-activated cell sorting
GAF	cGMP-specific phosphodiesterases, adenylyl cyclases and FhlA
GTP	guanosine triphosphate
H^{+}	proton
ICP-OES	inductively coupled plasma optical emission spectrometry
K^{+}	potassium
K_0	K^{+}-free minimal media
Li^{+}	lithium
LR	leader region
Na^{+}	sodium
NADH	nicotinamide adenine dinucleotide
NH_4^{+}	ammonium
PEP	phosphoenolpyruvate
PMF	proton motive force
PO_4^{3-}	phosphate

PTS	phosphotransferase system
PTS^{Ntr}	nitrogen-related phosphotransferase system
Rb^+	rubidium
RCK_C	regulator of conductance of K^+
RD	receiver domain
RNA	ribonucleic acid
RNAP	RNA polymerase
TCS	two-component system
USP	universal stress protein
wt	wild type
xyl	xylose

Introduction

1 Physiological roles of K^+

Potassium (K^+) plays a key role in maintaining vital functions in all domains of life. Living cells usually maintain this alkali metal at a concentration higher than 100 mM, ranking it as the most abundant of all intracellular cations [1,2]. This accounts for a very ancient decision of primitive cells to maintain high levels of K^+ in the cytoplasm while excluding sodium (Na^+) [1,2]. The abundance of K^+ within cells contributes considerably to set a negative transmembrane potential by counteracting the large negative charge of membrane lipids and nucleic acids [2–4]. Most organisms use K^+ as their main osmotic solute, they regulate its transport to balance osmolarity between the inside and outside of cells. K^+ thereby acts as an osmoprotectant and regulates turgor pressure to prevent cells from shrinking or bursting under osmotic stress [1,2]. On top of that, K^+ serves as the primary monovalent cation accompanying proton movement through both K^+/H^+ symporters and antiporters and thereby regulates intracellular pH[1,2].

Furthermore, K^+ is essential to some core cellular processes including splicing, translation and protein folding. Accordingly, key enzymes such as the translation factor EF-Tu [5], recombinase RadA [6], chaperonin GroEL [7] or pyruvate kinase [8] are K^+-dependent. Studies showed that two classes of ribozymes display specific K^+-binding sites, considered as critical to catalyse RNA splicing [9–11]. This property to bind nucleic acid and stabilize RNA folds further enables K^+ to take part in the ribosome's architecture [2,3,12]. Two K^+ ions have been shown to coordinate conformational arrangements within the decoding centre and x-ray structures identified another K^+ ion located in the peptidyl transferase centre [2,12,13]. Additionally, many GTPases critical to the translation process exert a K^+-dependent activation of GTP hydrolysis [2].

K^+ transport and its underlying regulations have been extensively studied in bacteria, mostly because K^+ is a critical modulator of virulence in several pathogens. It was demonstrated in *Pectobacterium wasabiae,* a phytopathogen, that the K^+-uptake system, Trk, is required for virulence induction [14]. Similarly, Trk has been reported essential for invasion and growth of *Salmonella* within epithelial cells. Impairment of K^+-transport resulted in a defective expression and secretion of effector proteins of Type III secretion system, thus reducing pathogenicity [15,16]. In addition, high K^+ environmental conditions were recently shown to promote host colonization by *Mycobacterium tuberculosis* [17].

Besides virulence, varied physiological processes are modulated by K^+ in bacteria [18–22]. In the Gram-positive bacterium *Bacillus subtilis,* K^+ has been involved in electrical communication, chemotaxis and biofilm formation [19,20]. Within biofilm communities, interior and peripheral cells communicate to ensure sufficient nutrient supply to the entire population. Upon nutrient limiting conditions, interior cells were shown to release intracellular K^+. Since each neighbouring cell in turn release K^+, the signal propagates as a wave in the biofilm. This long-range electrical communication would allow peripheral cells to reduce their nutrient uptake thereby guaranteeing nutrient access for interior cells [19]. Furthermore, emission of K^+ by *B. subtilis* biofilms has been shown to attract free motile cells, presuming a possible chemoattraction that participates in the formation of the biofilm [20]. The latter mechanism operates regardless of the species since the Gram-negative bacterium *Pseudomonas aeruginosa*, was also attracted to *B. subtilis* biofilms. This suggests that K^+-based electrical signalling

might be universal in bacterial communities. A study conducted in the symbiotic bacterium, *Sinorhizobium meliloti*, reported that K^+ is not only important for osmoadaptation and osmotolerance but also for the establishment of symbiosis with leguminous plants [23]. Impairment of K^+ uptake resulted in delayed formation of root nodules. In addition, in *Serratia sp.,* K^+ has been shown to affect motility, flotation and antibiotic production[24].

These works support the importance of K^+ as modulator of bacterial physiology and behaviour, yet, its relationship with the bacterial cell cycle remains uncharacterized. In eukaryotic cells, the role of K^+ in the cell cycle is often associated with turgor pressure and membrane potential [25–28]. Turgor pressure is known to contribute to the expansion of cell volume in growing cells. This has been extensively studied in plants for which K^+ is a major macronutrient. An increase in turgor pressure mediated by K^+ uptake is required for the G1 to S phase transition. In contrast, K^+ efflux decreases turgor pressure and enables cell division [26]. K^+-mediated variations in cell volume along the cell cycle were also reported in animal cells [29]. K^+ fluxes are accompanied by fluctuations in membrane potential throughout cell cycle [25,30]. At the limit between G1 and S phases, membrane potential is maintained at hyperpolarized values, thus providing the driving force for the entry of Ca^{2+} in the cell [31,32]. Since Ca^{2+} is an important mediator of cell division, its entry greatly contributes to cell cycle progression particularly through the expression and activation of cell cycle proteins [31,33].

K^+ channels, especially voltage gated, are held responsible for K^+ fluxes occurring along the cell cycle in eukaryotes [25,28,34]. Interestingly, numerous bacteria do not encode recognizable K^+ channels, although retaining active K^+-uptake systems [35]. Besides, unlike eukaryotic cells, the majority of K^+ channels found in prokaryotes are not voltage-dependent [34,35]. The bacterial cell cycle may therefore not be subject to the same K^+-dependent regulation.

2 K^+ transport

2.1 K^+ uptake systems

So far, five K^+ uptake systems have been reported in bacteria: Trk, Ktr, Kup, KimA and Kdp [1,2]. The classification of Trk and Ktr as transporters has however been recently challenged by crystal structures and biophysical studies arguing for a function of ion channel [36–40]. Most species possess at least two K^+ uptake systems; for instance *Staphylococcus aureus* harbors Ktr and Kdp [41] while *E. coli* and *Salmonella* both carry Trk, Kup and Kdp [1,42].

It is noteworthy to add that the two heavier alkali metals, rubidium (Rb^+) and caesium (Cs^+) are important inhibitors of K^+ uptake. This accounts for the similar organization of water molecules constituting the first hydration shell of these three ions [2]. Consequently, both Rb^+ and Cs^+, otherwise rarely involved in cellular processes, contaminate K^+-related functions. By competing for transport, Cs^+ was shown to limit K^+ uptake consequently inhibiting plant growth [2]. Both, Rb^+ and Cs^+ can nonetheless substitute the counterion function of K^+ since they have similar neutralizing activity [2].

Trk

The Trk system is the most widely spread among bacterial species. It transports K^+ with a low affinity ($K_m \approx 1$ mM) probably in symport with a proton. Ru^+ is also a substrate of Trk but it is transported at a 10-fold lower rate [1]. This system is composed of transmembrane proteins providing the path for K^+, TrkH/G [37] and two cytosolic proteins, TrkA and TrkE regulating K^+ flux [1,32]. TrkA binds both NADH and

ATP with high affinity, but only ATP binding induces conformational changes leading to gate opening of TrkH/G [38,40].

Ktr

The closely related Ktr system is found in several bacteria including *B. subtilis* [43], *S. aureus* [44] or *Vibrio alginolyticus* [45]. The two proteins constituting this system in most bacteria, KtrA and KtrB, are distant relatives of TrkA and TrkH respectively. Some bacteria including *B. subtilis* possess two Ktr systems differing by their affinities for K^+ : KtrAB ($K_m \approx 1$ mM) and KtrCD ($K_m \approx 10$ mM) [1,22,43].

Kup

The KUP family brings together a whole range of proteins including the *E. coli* Kup, which is certainly the best characterized so far [46–48]. The latter is a single membrane protein showing moderate affinity for K^+ ($K_m \approx 0.5$ mM) [42,46]. Unlike other systems, Kup does not strongly distinguish K^+ from the two heavier alkali cations [49] and is actually the only path for specific Cs^+ transport in bacteria [49]. Kup proteins are suggested to operate as a K^+/H^+ symporters [50].

KimA

The newly discovered *B. subtilis* K^+ importer A (KimA) [51] has now been classified in the KUP family. Homologs of KimA have been found in firmicutes, actinobacteria and proteobacteria [51]. KimA is structurally similar to *E. coli* Kup and residues crucial to its K^+/H^+ symporter function are fully or highly conserved among KUP members [47]. Yet, KimA shows a higher affinity for K^+ [51].

Kdp

Kdp is the system displaying the highest affinity for K^+ with a K_m in the micromolar range [42]. In *E. coli*, this inner membrane complex, also called KdpFABC, is constituted of four subunits all encoded in the same operon (Fig. 1). KdpF primarily serves a structural role and stabilizes the complex, it is absent in some species. KdpA is a channel-like subunit composed of ten transmembrane segments. Four helices protruding within its pore act as the selectivity filter for K^+ [52]. While KdpA provides the path for K^+, the energy required for its transport is supplied by KdpB operating as a P-type ATPase [52,53]. KdpC is suggested to act as a catalytic chaperone by increasing the ATP-binding affinity of KdpB [54,55].

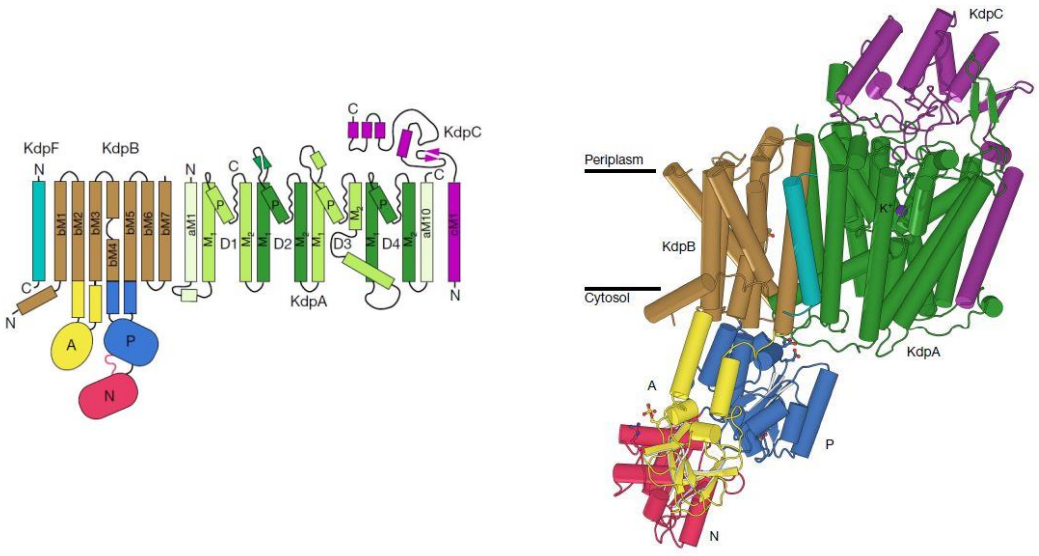

Figure 1. Transmembrane topology of the KdpFABC complex in *E. coli*.
KdpF (cyan) is a single transmembrane helix. KdpA (green) harbours a K^+ ion bound in its centre (purple sphere). KdpB is comprised of a transmembrane domain (brown) and three cytoplasmic domains found in all P-type ATPases involved in nucleotide binding (N, red), phosphorylation (P, blue) and dephosphorylating actuator (A, yellow). KdpC (purple) possesses a single transmembrane helix and a periplasmic soluble domain (Figure adapted from Huang et *al.,* 2017).

Expression of Kdp is regulated by the KdpD/E two-component system (TCS), which is encoded adjacent to *kdpFABC* in most organisms [56,57]. Like most histidine kinases (HK), KdpD is a homodimeric transmembrane protein harbouring both DHp (Dimerization Histidine phosphotransfer) and CA (Catalytic ATP-binding) domains [58,59]. It displays four transmembrane segments and consequently two periplasmic loops suggested to be involved in signal sensing [59]. On the other hand, the response regulator (RR) KdpE typically comprises a receiver domain (RD) and a DNA-binding domain (DBD) [58]. Once phosphorylated, KdpE dimerizes and activates *kdpFABC* expression [1,60].

When K^+ becomes limiting, KdpD autophosphorylates and transfers its phosphoryl group to KdpE which subsequently initiates transcription of the *kdp* operon. Also exhibiting a phosphatase activity, KdpD ultimately dephosphorylates KdpE~P. As a result, Kdp is highly expressed in low K^+ conditions, precisely when other transport systems are unable to take up K^+ efficiently [1,61].

The exact signal activating KdpD remains largely controversial [61,62]. It was long thought that turgor pressure was directly sensed by KdpD but this hypothesis has now been refuted [63–65]. While other signals such as intracellular Na^+ and NH_4^+ have been proposed [63,66], a recent study provided strong evidence arguing for a dual sensing of extra- and intracellular K^+ in *E. coli* [59].

Both enzymatic activities of the bifunctional KdpD were shown to be independently regulated by K^+ (Fig. 2). Whereas the kinase activity was inhibited by extracellular K^+, phosphatase activity was stimulated by intracellular K^+. Four amino acids located in the second periplasmic loop were identified as a K^+-specific recognition site. Substitution of those four amino acids by alanine resulted in a strain unable to sense extracellular K^+. In contrast, the K^+-recognition site for intracellular sensing remains to be identified. Whilst specific residues could not be highlighted, the C-terminal cytoplasmic domain of KdpD was shown sufficient to retain a K^+-dependent phosphatase activity [59,67]. Although this has yet to be experimentally investigated, authors suggested that the cytoplasmic GAF domain of KdpD may be responsible for intracellular K^+ sensing (Fig. 2 and Fig. 10A). Most GAF domains are involved in regulatory functions through binding to cyclic nucleotides, however, they are also known to bind other ligands including ions [68,69].

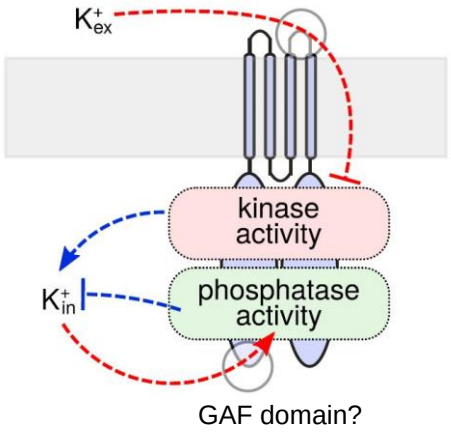

Figure 2. Dual sensing by the sensor kinase KdpD in *E. coli*.

Extracellular K^+ is sensed in the second periplasmic loop of KdpD and inhibits its kinase activity. On the other hand, intracellular K^+ activates its phosphatase activity. The latter recognition site remains to be identified but intracellular K^+ sensing is believed to take place in the C-terminal cytoplasmic domain, perhaps via the GAF domain of KdpD. This dual sensing integrating both the supply and the demand provides robust cellular homeostasis (Figure adapted from Schramke et *al.*, 2016).

This dual sensing regulating both activities of KdpD provides robust homeostasis in changing environments [59]. Unlike single sensing, this optimized strategy enables to sense simultaneously both the supply and the demand, thus providing a tight regulation of *kdpFABC* expression. As long as intracellular K^+ concentrations remain sufficient for all cellular processes, KdpD phosphatase activity prevents *kdpFABC* expression despite kinase activation upon K^+ limitation [59]. Additionally, in non-limiting environments, a rapid growth rate can deplete the intracellular K^+ pool despite its abundance outside cells. In such conditions, K^+ uptake is fine tuned in order to meet the intracellular requirements [59].

2.2 K^+ channels

Prokaryotic K^+ channels have mostly been studied to extend the knowledge of their eukaryotic counterparts. Although the research around their physiological role has been neglected, prokaryotic K^+ channels were shown to participate in electrical signalling, information propagation, and intercellular communication [19,20,32]. K^+ channels are likely not involved in K^+ uptake. Depriving *E. coli* of its unique K^+ channel Kch has no detectable effect on growth [35,70]. It has been suggested that they might adjust membrane potential *in vivo*, nonetheless, supporting evidence remains rather limited.

2.3 K^+ efflux

Two arguments account for the physiological requirement of K^+ efflux: the necessity to maintain a negative membrane potential and the need to reduce excessively high turgor pressure upon osmotic stress[1].

Like other Gram-negative bacteria, *E. coli* carries two K^+ efflux systems named KefB and KefC each associated with a soluble protein necessary to their activity [1,71,72]. Those ligand-gated channels predominantly serve as emergency systems to deal with toxic compounds [1,73]. Their gates are maintained in closed state by gluthatione, acting as an inhibitory ligand. Facing toxic compounds, gluthatione forms adducts that promote K^+ efflux through KefB and KefC. K^+ efflux is accompanied by a decrease in intracellular pH since KefB and KefC operate as K^+/H^+ antiporters. The cytoplasm acidification resulting from K^+ release reduces the amount of lethal lesions generated by the toxins [73].

Upon sudden turgor increase, rapid K^+ efflux is carried out by mechanosensitive channels in a non-specific manner. The pressure needed for those channels to open increases with their size [1]. Systems evacuating K^+ when turgor increases more slowly remain to be described[1].

3 Regulatory mechanisms affecting K^+ transport

3.1 PhoR/B-mediated regulation

In *E. coli*, a bidirectional crosstalk has been reported between KdpD/E and PhoR/B, another TCS involved in phosphate limitation [74] (Fig. 3). *In vitro* phosphotransfer assays showed that KdpE can be phosphorylated not only by KdpD but also by the HK PhoR. In the absence of KdpD, the phosphorylation of KdpE by PhoR was shown to activate *kdpFABC* expression. Consistent with this idea, *kdpFABC* expression was enhanced under phosphate limitation. On the other hand, the RR PhoB can be phosphorylated by KdpD and K^+ limitation has been shown to enhance expression of the *pho* regulon. K^+ had been previously shown to be important for phosphate uptake but the underlying

molecular mechanisms had not been uncovered yet [75]. It was reported in *E. coli* that low K^+ conditions decreased phosphate uptake and intracellular levels of inorganic phosphate, both immediately restored upon addition of K^+ [75]. This cross-regulation connecting phosphate and K^+ homeostasis highlights a possible explanation. Also, this mechanism accounts for a fine-tuning of the ratio between positively and negatively charged ions inside the cell [74].

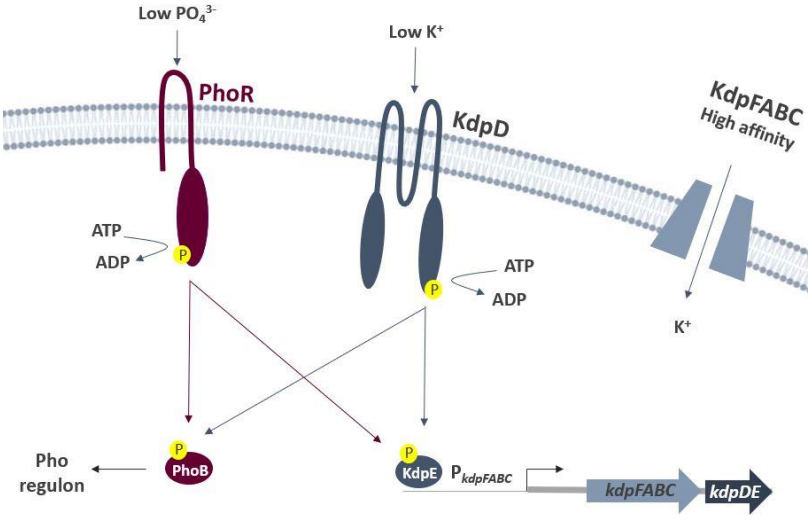

Figure 3. Bidirectional crosstalk between KdpD/E and PhoR/B two-component systems in *E. coli*.

Activated under phosphate limitation, the sensor kinase PhoR can transfer its phosphoryl group to both RRs PhoB and KdpE, subsequently activating transcription of the *pho* regulon and the *kdpFABC* operon respectively. Conversely, low K^+ conditions activate KdpD which thereby phosphorylates not only KdpE but also PhoB. (Figure adapted from Schramke *et al.*, 2017)

3.2 PTS^{Ntr}-mediated regulation

Several studies showed that the so-called nitrogen phosphotransferase system (PTS^{Ntr}) controls K^+ homeostasis by acting on Kdp expression and Trk activity (Fig. 4) [76–79]. PTS^{Ntr} works in parallel with the cognate sugar phosphotransferase system (sugar PTS) involved in carbohydrates uptake. In this phosphotransfer chain, a phosphoryl group is transferred from phosphoenolpyruvate (PEP) to sugar PTS components successively: Enzyme I (EI), HPr and Enzyme II (EII). One organism can carry diverse EII complexes as they refer to sugar-specific transporters which ultimately phosphorylate their substrates during uptake. Sugar PTS communicates through phosphoryl exchange with the regulatory PTS^{Ntr} whose equivalent components are EI^{Ntr}, NPr and EIIA^{Ntr} [78]. Utilization of a rich carbon source such as glucose favours the dephosphorylation of both Sugar PTS and PTS^{Ntr} components. On one hand, unphosphorylated EIIA^{Ntr} has been also shown to interact with TrkA. This interaction inhibits K^+ uptake through Trk in high K^+ conditions (> 5 mM)[79]. On the other hand, the unphosphorylated form of EIIA^{Ntr} was shown to directly interact with KdpD, stimulating its kinase activity. In low K^+ conditions (< 5 mM), this interaction promotes elevated levels of KdpE~P and subsequently increases transcription of *kdpFABC.* PTS^{Ntr} appears to mediate K^+ homeostasis by avoiding both K^+ depletion and K^+ surplus. It does so by stimulating *kdpFABC* expression in low K^+ conditions and by inhibiting Trk-mediated K^+ uptake in high K^+ conditions [76].

Likewise, EIIA^{Ntr} also activates the sensor kinase PhoR upon phosphate limitation. This shared regulatory mechanism reinforces the previously described connection between phosphate and K^+ homeostasis[80].

It was later discovered that this control underlies a deeper mechanism of regulation: PTS^{Ntr} regulates sigma factor selectivity by modulating K^+ levels. The competition between σ^{70} and σ^S for interaction with the RNA polymerase (RNAP) is influenced by K^+ intracellular levels [77]. *In vitro* transcription assays

were performed in the presence of different K^+ concentrations ranging from 100 to 500 mM. As K^+ concentrations scaled up, the transcription of σ^{70}-dependent genes and σ^S-dependent genes were respectively decreased and increased. Additionally, in high K^+, the amount of σ^{70} and σ^S bound to core RNAP were respectively decreased and increased.

This modulation of sigma factor selectivity has been proposed as a mechanism for coping with stress conditions. Depending on the phosphorylation state of $EIIA^{Ntr}$, the resulting K^+ intracellular levels preferably favour the binding of σ^{70} or σ^S to the core RNAP [77]. Identifying the signal controlling the phosphorylation of PTS^{Ntr} components would help to better understand this regulation.

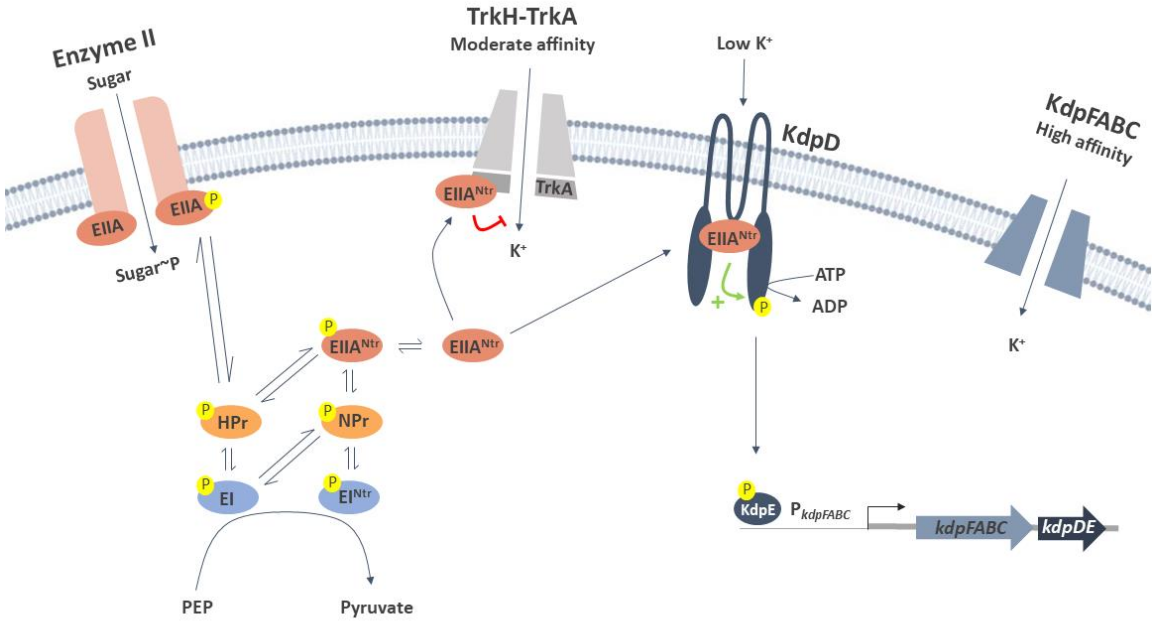

Figure 4. PTS^{Ntr}-mediated regulation of K^+ homeostasis in *E. coli*.
Carbohydrate uptake through sugar PTS is initiated by the translocation of a phosphoryl group PEP to EI. The latter thereby transfers the phosphoryl group to HPr and EII which ultimately phosphorylates their substrate during uptake. Components of the sugar PTS can phosphorylate members of the regulatory PTS^{Ntr} system working in parallel. In high K^+ conditions (> 5 mM), the unphosphorylated form of $EIIA^{Ntr}$ inhibits Trk-mediated K^+ uptake by interacting with its gating protein, TrkA. In addition, unphosphorylated $EIIA^{Ntr}$ interacts with KdpD and stimulates its kinase activity in low K^+ conditions (<5 mM). This results in higher levels of KdpE~P and enhanced transcription of the *kdpFABC* operon encoding the high-affinity K^+ uptake system. (Figure adapted from Pflüger-Grau & Görke, 2010)

3.3 c-di-AMP-mediated regulation

Over the past few years, increasing evidence has appointed the second messenger c-di-AMP as a new regulator of K^+ homeostasis in Gram-positive bacteria [51,81–84]. It exerts a dual control by interacting directly with both transport and regulatory proteins and by binding to a regulatory RNA known as a riboswitch.

K^+ transport through Ktr, KimA and Kup is inhibited by direct binding of c-di-AMP. Affinity pull-down assays and differential radial capillary action ligand assays (DRaCALA) identified KtrA, KimA and two Kup transporters as c-di-AMP binding proteins in *S. aureus* [44,85], *B. subtilis* [82] and *Lactococcus lactis* [48] respectively. Studies showed that c-di-AMP interacts with KtrA through its RCK_C domain (regulator

of conductance of K^+) and ultimately inhibits Ktr-mediated K^+ uptake [44,85]. Carried by several c-di-AMP binding proteins, the presence of this conserved RCK_C domain in other transporters might suggest a c-di-AMP dependent regulation [85].

Besides interacting with K^+ transporters, c-di-AMP has been reported to bind the *S. aureus* KdpD sensor kinase. A conserved motif ($SXSX_{20}$-FTAXY) located in the cytoplasmic region was identified as the c-di-AMP binding pocket. High levels of c-di-AMP inhibit the KdpD-dependent upregulation of the *kdpFABC* operon. This suggests that the binding of c-di-AMP to KdpD disturbs the signalling of the TCS through a yet unknown mechanism [81].

On top of this, c-di-AMP controls the expression of genes encoding K^+ transporters by a c-di-AMP-dependent riboswitch. The 5' leader region (LR) of the *B. subtilis kimA* transcript can adopt two mutually exclusive conformations: one favours transcription readthrough while the other promotes transcription termination [86]. Upon direct binding of c-di-AMP, the *kimA* 5' LR preferentially forms a structure exposing a predicted intrinsic transcription terminator. It therefore inhibits transcription elongation of *kimA* (Fig. 5). This type of regulation involving premature termination of transcription is commonly referred to as attenuation [87]. Interestingly, a study showed that transcription levels of *kimA* were higher in low K^+ conditions (0.1 mM KCl) than in high K^+ conditions (5 mM KCl) [51]. Indeed, the high-affinity K^+ transporter KimA was exclusively detectable in low K^+ conditions. This K^+-dependent control of *kimA* expression is suggested to be achieved through a modulation of c-di-AMP intracellular levels. Supporting this hypothesis, concentrations of c-di-AMP were increased by two-fold in high K^+ conditions. c-di-AMP is exclusively required in high K^+ conditions since a strain lacking c-di-AMP synthesising genes is viable in low but not in high K^+ conditions. Expression of both Ktr and Kdp systems is likely controlled by a similar mechanism since this conserved c-di-AMP riboswitch was also found upstream the *ktrAB* [86] and *kdpFABC* [84] operons in *Bacillus* species.

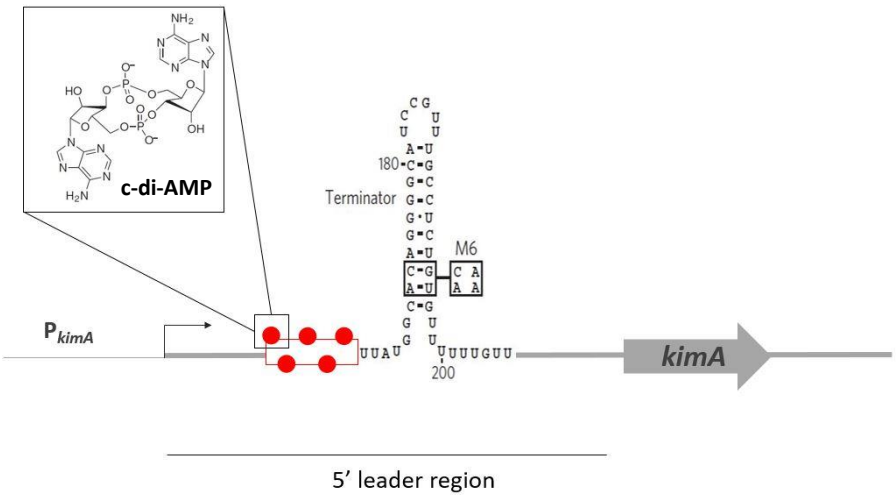

Figure 5. Expression of *kimA* is controlled by a c-di-AMP riboswitch in *B. subtilis*.
The binding of c-di-AMP to the 5' leader region of the *kimA* transcript favours the formation a stem loop predicted to be an intrinsic transcription terminator. The transcription of *kimA* is therefore terminated upon c-di-AMP binding (Figure adapted from Nelson et *al.,* 2013).

Altogether, c-di-AMP arises as a negative regulator of K^+ uptake by acting on various levels. This is consistent with the fact that intracellular concentrations of c-di-AMP are varying along with that of K^+. However, to be physiologically relevant, c-di-AMP-mediated negative regulation should primarily

affect high-affinity uptake systems. It could be hypothesized that KimA and KdpD bind c-di-AMP with a higher affinity than other c-di-AMP binding proteins and/or that both *kimA* and *kdpFABC* riboswitches display small variations in sequence improving c-di-AMP binding.

4 *Caulobacter crescentus* and its relationship with K^+

Caulobacter crescentus is the ideal organism to address the role of K^+ in the regulation of bacterial cell cycle. This aquatic α-proteobacterium is a renowned model to study cell cycle and its regulations. It divides asymmetrically into two morphologically distinctive daughter cells: a sessile stalked cell and a flagellated swarmer cell (Fig. 6) [88]. While the stalked cell directly initiates DNA replication at birth, the non-replicative swarmer cell primarily goes through a pre-replicative (G1) phase before differentiating into a stalked cell. Upon stress conditions, such as nitrogen and carbon starvation, the swarmer-to-stalked differentiation is delayed and the G1/swarmer phase is consequently extended [89–91]. Since the swarmer cell is motile and chemotactically active, this emerges as a strategy to promote colonization of more suitable environments.

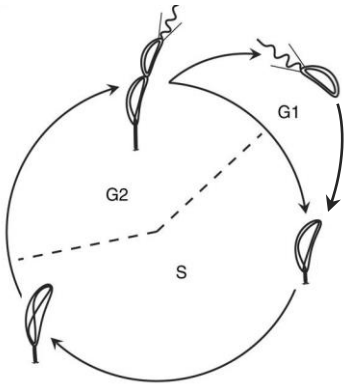

Figure 6. *Caulobacter crescentus* cell cycle.

Asymmetric cell division of *C. crescentus* results in two morphotypes: a stalked cell directly entering S phase and a swarmer cell going through a G1 phase before differentiating and replicating (Figure adapted from Ronneau *et al.*, 2016).

Protein blasts searches have identified Kup and Kdp homologous proteins in *C. crescentus*, predicting that those two systems are participating in K^+ uptake in this species. In addition, *C. crescentus* possesses a putative K^+ channel (CCNA_01688) sharing only 12% and 15% identity with Kch from *E. coli* and KcsA from *Streptomyces lividans*, respectively. This putative K^+ channel harbours nonetheless a TrkA-like regulatory domain, present in some K^+ channels [19] and the conserved K^+-selectivity filter sequence. Homologs of the two K^+ efflux systems, KefB and KefC, are also present in *C. crescentus*.

Unsurprisingly for a Gram-negative α-proteobacterium, the genome of *C. crescentus* does not encode any predicted c-di-AMP synthase enzymes. In contrast, both PhoR/B TCS and PTS^{Ntr}, described to regulate of K^+ transport in *E. coli*, have been studied in *C. crescentus*.

The PhoR/B TCS that responds to phosphate limitation is conserved in *C. crescentus* and the genome-wide PhoB binding targets have been identified under starved and un-starved phosphate conditions [92]. A part of the PhoB regulon in *C. crescentus* turns out to be conserved with *E. coli*. For instance, phosphorylated PhoB was able to efficiently bind to the promoter regions and to drive the expression of *pstCAB* and *pstS* genes, which encode a high-affinity phosphate transporter. Nevertheless, important differences were revealed with *E. coli* PhoB regulon, which demonstrates the evolutionary plasticity of transcriptional responses driven by conserved RRs.

The PTS^{Ntr} in *C. crescentus* has recently been thoroughly characterized, specifically on account of its contribution to the response to nitrogen starvation [89]. Members of the PTS^{Ntr} in *C. crescentus* include

EI^{Ntr}, a unique HPr homologue and $EIIA^{Ntr}$. Nitrogen starvation is signalled through the PTS^{Ntr} by the way of sensing intracellular glutamine levels. Binding of glutamine to the GAF domain of EI^{Ntr} inhibits its phosphorylation. Therefore, glutamine deprivation promotes the phosphorylation of EI^{Ntr} and its downstream PTS^{Ntr} components, HPr and $EIIA^{Ntr}$. Phosphorylation of PTS^{Ntr} components results in the accumulation of an alarmone, called (p)ppGpp, thereby dictating the response to nitrogen starvation. An accumulation of (p)ppGpp can be achieved by altering its synthesis and/or its degradation [93]. The genome of *C. crescentus* encodes a single (p)ppGpp synthetase/hydrolase, named SpoT, whose enzymatic activities were shown to be modulated by both phosphorylated HPr and $EIIA^{Ntr}$ [89]. On one hand, phosphorylated $EIIA^{Ntr}$ directly interacts with SpoT to inhibit its hydrolase activity. On the other hand, phosphorylated HPr stimulates the SpoT synthetase activity through a yet unknown mechanism.

Objectives

Mounting evidence denotes K^+ as an important modulator of bacterial physiology, which regulates multiple processes including biofilm formation, chemotaxis, cell to cell communication, virulence, *etc.* However, little is known about its relationship with the bacterial cell cycle nor about its fundamental role in free-living environmental bacteria such as the α-proteobacterial oligotroph *Caulobacter crescentus*.

The aim of this master thesis is to assess the potential role played by K^+ in regulating cell cycle progression in *C. crescentus* and to gain insights on actors contributing to this regulation. To that end, we will track cell cycle progression by monitoring DNA content of synchronous populations via flow cytometry analysis. The role played by the conserved high-affinity K^+ transporter Kdp as well as its regulation driven by the KdpD/E TCS will be studied.

Material & Methods

Bacterial strains and growths conditions

All *Escherichia coli* strains used in this thesis were grown aerobically in Luria-Bertani (LB) broth (Sigma). *E. coli* Top10 was used for cloning purpose while *E. coli* MT607 was used for triparental matings. Thermo-competent cells were used for transformation of *E. coli*. All *Caulobacter crescentus* strains used are derived from the synchronizable wild-type strain NA1000. The traditional synthetic media supplemented with glucose (M2G) was modified by replacing potassium salts by their equivalent sodium salts to obtain a medium without any K^+ (K_0) to which the desired K^+ concentrations could be added. The source of K^+ consists in both KH_2PO_4 and K_2HPO_4 mixed to an equivalent ratio in terms of K^+ concentration. For each experiment, cells were first grown at 30 °C; in Peptone Yeast Extract (PYE), then adapted overnight at 30 °C in K_0 media supplemented with 0.5 mM K^+, washed twice in K_0 media and finally grown at 30 °C in K_0 media supplemented with the desired K^+ concentration. For growth curve measurements, cultures were diluted to a final OD_{660} of 0.02 in a 96-well plate. Growth was monitored during 48 h with continuous shaking at 30 °C, in an automated plate reader (Bioscreen C, Lab Systems) measuring OD_{660} every 10 min. For *E. coli*, antibiotics were used at the following concentrations (µg/ml; in liquid/solid medium): chloramphenicol (20/30), kanamycin (30/50), oxytetracycline (12.5/12.5), spectinomycin (100/100), streptomycin (50/100) while for *C. crescentus*, media were supplemented with kanamycin (5/20), oxytetracycline (2.5/2.5), nalidixic acid (20) when appropriate. Genes under the control of the inducible xylose promoter (P_{xylX}) were induced with 0.1 % xylose.

Construction of plasmids and strains

Single mutations were created by oligonucleotide-directed mutagenesis and introduced using pNPTS138 recombinant plasmid. Around 500 base pairs upstream and downstream the targeted mutation were respectively amplified using primer couple for1/rev1 and for2/rev2. Both PCR products and pNPTS138 were cut with adequate restriction enzymes to perform a triple ligation. Subsequent pNPTS138-derivative plasmids were introduced in *E. coli* Top10 by heat-shock transformation.

After triparental mating, integration of pNPTS138-derivative plasmids in the chromosome by single homologous recombination was selected on plates containing kanamycin. Two independent recombinant clones were inoculated in PYE medium without kanamycin and incubated overnight at 30 °C. Dilutions were subsequently spread on PYE plates containing 3 % sucrose and incubated at 30 °C. Around 40 colonies were picked and patched on PYE plates with and without kanamycin. Kanamycin-sensitive clones, which had lost the integrated plasmid due to a second recombination event, were then tested by PCR on colony and the point mutation was verified by sequencing.

The plasmid used for *kdpD* complementation was constructed by amplifying the *kdp* promoter together with *kdpD* in a Δ*kdpABC* background. The *kdp* promoter sequence amplified represents around 400 base pairs upstream the start codon of the operon. Plasmids used for complementation and β-galactosidase assays were introduced by triparental mating and transformants were selected on plates with adequate antibiotic.

Oligonucleotides used in this thesis.

Name	Description	5' to 3' sequence
RH2034	Rev *kdpD* STOP	ggatccccgggtactgcagtcatagcaggtgatgcggcgtcgtg
RH2171	For P_{kdp}	ttagttacttaggggtaccctggatcagcgacaggtcgg
RH2172	Rev P_{kdp}	cctaagtaactaaaagcttggaattggtccgtcagaacttgtcg
RH2384	For 3' Twin-strep tag KdpE	ttagttacttaggcatatgatgagcgcgcttcgccaccgcat
RH2385	Rev 3' Twin-strep tag KdpE	cctaagtaactaagtcgactggagccgatagcctacgccagg
RH2588	For1 $kdpD_{H670N}$	acgcgtcacggccgaagctaaaagtgtttctgggcatgg
RH2589	For 2 $kdpD_{H670N}$	tgaactcggtcagcaatgacctgcgcacgc
RH2590	Rev1 $kdpD_{H670N}$	gcgtgcgcaggtcattgctgaccgagttca
RH2591	Rev2 $kdpD_{H670N}$	gcaggatatctggatccacaggtgatgcggcgtcgtga
RH2592	For 1 $kdpE_{D56E}$ and $kdpE_{D56A}$	acgcgtcacggccgaagctaacgatgaaccgcaaatccat
RH2593	For 2 $kdpE_{D56A}$	tggtgctggctctgggcttgcccgacat
RH2594	Rev 1 $kdpE_{D56A}$	atgtcgggcaagcccagagccagcacca
RH2595	Rev2 $kdpE_{D56E}$ and $kdpE_{D56A}$	gcaggatatctggatccaccctggagccgatagcctacg
RH2596	For2 $kdpE_{D56E}$	tggtgctggaactgggcttgcccgacat
RH2597	Rev1 $kdpE_{D56E}$	atgtcgggcaagcccagttccagcacca
RH2764	For screening oligo $kdpD_{H670N}$	gctcggctctgatgaactcggtcaggaa
RH2765	For screening oligo $kdpE_{D56A}$	cgacgccgtggtgctgtct

Plasmids used in this thesis.

Name	Description	Reference/Source
pHR253	pNPTS138 (kanamycin^R)	Our lab
pHR566	pXC-5 (oxytetracyclin^R)	Our lab
pHR664	pMR10 (kanamycin^R)	Shapiro, L.
pHR853	pMCS-1-Twin-Strep-3' (spectinomycin^R, streptomycin^R)	Our lab
pHR1257	pXC-5 *kdpE* Twin-strep (C-term) (oxytetracyclin^R)	This thesis
pHR1258	pNPTS138 $kdpE_{D56E}$ (kanamycin^R)	This thesis
pHR1259	pNPTS138 $kdpE_{D56A}$ (kanamycin^R)	This thesis
pHR1260	P_{kdp}*::lacZ* fusion on pRKlac290 (oxytetracyclin^R)	This thesis
pMC5	P_{kdp}*::kdpD* fusion on pMR10 (kanamycin^R)	This thesis
pMC6	pNPTS138 $kdpE_{H670N}$ (kanamycin^R)	This thesis

Strains used in this thesis.

Name	Description and relevant genotype	Reference/Source
RH317	DH10B pNPTS138	Our lab
RH319	MT607 helper strain	Our lab
RH322	DH10B pMR10	Shapiro, L.
RH610	DH5α pRKlac290 P_{pilA}*::lacZ*	[94]
RH783	Top10 Thermocompetent cells	[95]
RH1486	Top 10 pXC-5	Our lab
RH3071	Top 10 pNPTS138 $kdpE_{D56E}$	This thesis
RH3072	Top 10 pNPTS138 $kdpE_{D56A}$	This thesis
RH3073	Top10 pRKlac290 P_{kdp}*::lacZ*	This thesis
RH50	Wild-type NA1000 strain	[96]

RH1752	NA1000 *spoT*$_{D81G}$	[89]
RH1755	NA1000 Δ*spoT*	[89]
RH2808	NA1000 Δ*kdpD*	Quintero-Y, A.
AQ34	NA1000 Δ*kdpABC*	Quintero-Y, A.
AQ39	NA1000 Δ*kdpE*	Quintero-Y, A.
MC11	NA1000 Δ*kdpD* pRKlac290 P$_{kdp}$*::lacZ*	This thesis
MC12	NA1000 Δ*kdpA-C* pRKlac290 P$_{kdp}$*::lacZ*	This thesis
MC13	NA1000 Δ*kdpE* pRKlac290 P$_{kdp}$*::lacZ*	This thesis
MC14	NA1000 pRKlac290 P$_{kdp}$*::lacZ*	This thesis
MC15	NA1000 Δ*kdpE* pXC-5 *kdpE* Twin-strep (C-term)	This thesis
MC19	NA1000 *kdpE*$_{D56E}$	This thesis
MC20	NA1000 *kdpE*$_{D56A}$	This thesis
MC21	NA1000 Δ*kdpD* pMR10	This thesis
MC22	NA1000 Δ*kdpD* pMR10 P$_{kdp}$*::kdpD*	This thesis
MC23	NA1000 pMR10	This thesis
MC28	NA1000 *kdpD*$_{H670N}$	This thesis
MC29	NA1000 *kdpD*$_{H670N}$ pRKlac290 P$_{kdp}$*::lacZ*	This thesis
MC31	NA1000 *kdpE*$_{D56A}$ pRKlac290 P$_{kdp}$*::lacZ*	This thesis

Cellular fractionation and determination of K^+ concentrations

Cells were grown in 30 ml of K_0 media supplemented with adequate K^+ concentrations and split into two tubes; one for the total fraction; the other for cellular fractionation. Cells were fixed in 2% paraformaldehyde for 20 min on ice, washed three times in ice cold wash buffer (10 mM TrisHCl pH 6.8; 100 µM EDTA) and centrifuged for 10 min at 8000 rpm; 4°C. For the total fraction, cells were resuspended in milli-Q water and passed twice through a French Press (LA Biosystems B.V. at 5.48 bar). For cellular fractionation, cells were resuspended in Zwittergent buffer (0.2 M Tris HCl pH 7.6). Then, 0.25 % ZWITTERGENT® was added and incubated at room temperature for exactly 10 min to solubilize the outer membrane exclusively. The suspension was centrifuged for 15 min at 14 500 rpm; 4 °C and the supernatant, corresponding to the periplasmic fraction, was gently isolated whereas the remaining pellet containing spheroplasts was resuspended in milli-Q water. The later cytoplasmic fraction was passed once through a French press. Samples of each of the three fractions were collected to verify the efficiency of the cellular fractionation by immunoblot.

K^+ concentrations were determined by ICP-OES (Inductively coupled plasma - optical emission spectrometry). Samples were diluted to a final concentration of 1M HNO_3 for analysis. Calibration was performed using $KHNO_3$ ICP standard solution (Carl Roth; Ref: 2425.1).

Flow cytometry analysis.

DNA content was assessed using fluorescence activated cell sorting (FACS). Cells were fixed in ice-cold 77% ethanol. Fixed samples were then washed in FACS staining buffer (10mM Tris pH 7.2, 1mM EDTA, 50mM NaCitrate, 0.01% Triton X-100) then incubated for 30 min at room temperature in FACS staining buffer containing 0.1 mg/ml RNaseA. Cells were then collected by centrifugation for 3 min at 9000 rpm, resuspended in 1ml FACS staining buffer containing 0.5 mM Sytox Green Nucleic acid stain

(Life Technologies), and incubated for 5 min at RT in the dark. Samples were analysed in flow cytometer (FACS Verse, BD Biosciences) at laser excitation of 488 nm. At least 1000 cells were recorded for each experiment. Before analysis, settings were adjusted with samples of a wild-type (RH50), a G1 accumulating strain (*spoT*$_{D81G}$, RH1752) and a G2 accumulating strain (Δ*spoT,* RH1755) grown in PYE. Data were analysed with the BD FACSuite V1.0.5 software.

Synchronization of cells

Cells were grown in 300 ml K_0 media supplemented with 0.5 mM K^+, harvested by centrifugation for 15 min at 6000 rpm, 4 °C; and resuspended in 45 ml of ice cold K_0 media combined with 20 ml of ice cold Ludox® (Sigma-Aldrich; Ref 420808). After inverting several times, the cell-Ludox suspension was centrifuged for 35 min at 9000 rpm, 4 °C. Swarmer cells, corresponding to the bottom band, were collected, washed twice in ice-cold K_0 media and finally resuspended in K_0 media supplemented with adequate K^+ concentrations for growth at 30 °C. Samples were withdrawn every 20 minutes for 140 min for FACS analysis.

β-galactosidase assays

Cultures were either grown to stationary phase directly in a 96-wells plate or grown in flasks from which samples were withdrawn throughout growth and placed at -80 °C in between time points. Permeabilization of cells was performed by incubating cells with lysis buffer (20 mg/ml polymyxin B, β-mercaptoethanol) for 30 min at 28 °C. Then, 50 µl of 4 mg/ml O-nitrophenyl-β-D-galactopyranoside (ONPG) were added. Lysis and ONPG solutions were prepared using Z buffer as a solvent (60 mM Na_2HPO_4, 40 mM NaH_2PO_4, 10 mM KCl, 1 mM $MgSO_4$, pH 7.0). Both OD_{420} and OD_{550} were measured every minute for 30 min at 30 °C using a fluorimeter (SpectraMax®, Molecular Devices). Miller Units were calculated using the following formula [97]:

$$\text{M.U.} = \frac{[OD_{420} - (1.75\ x\ OD_{550})]x\ 1000}{OD660x\ t\ x\ v}$$

where t is the reaction time in min

v is the volume of culture used in ml

Proteins purification

In order to immunize rabbits for production of polyclonal antibodies, an *E. coli* BL21 (DE3) pLysS strain carrying plasmid pET-28a-*kdpE* was grown in LB medium supplemented with kanamycin and chloramphenicol until an OD600 of 0.5. After addition of IPTG to a final concentration of 1 mM, the culture was incubated at 18 °C for 18 h. Cells were then harvested by centrifugation for 30 min at 5,000 x g, 4 °C. The pellet was resuspended in 20 ml of binding buffer (20 mM Tris-HCl pH 8.0, 500 mM NaCl, 10% glycerol, 10 mM $MgCl_2$, 12.5 mM Imidazole) supplemented with complete EDTA-free protease cocktail inhibitor (Roche), 400 mg lysozyme (Sigma) and 10 mg DNaseI (Roche) and incubated for 30 min on ice. Cells were then lysed by sonication. After centrifugation at 12,000 rpm for 30 min at 4°C, the lysate was loaded on a Ni-NTA column and incubated 1 h at 4 °C with end-over-end agitation. The column was then washed with 5 ml binding buffer, 3 ml Wash1 buffer (binding buffer with 25 mM imidazole), 3 ml Wash2 buffer (binding buffer with 50 mM imidazole), 3 ml Wash3 buffer (binding buffer with 75 mM imidazole). Proteins bound to the column were eluted with 3 ml Elution buffer (binding buffer with 100 mM imidazole) and aliquoted in 300 µl fractions. All

the fractions containing the protein of interest (checked by Coomassie blue staining) were pooled and dialyzed in Dialysis buffer (20 mM Tris pH 8, 500mM NaCl, 10% glycerol).

Western blot analysis

To prepare protein crude extracts, cells in exponential phase were pelleted and resuspended in SDS-PAGE loading buffer. Cells were then lysed by incubation for 10 min at 95 °C. Samples were loaded and subjected to electrophoresis in a 12% SDS-polyacrylamide gel. Proteins were transferred onto a nitrocellulose membrane then blocked overnight at 4°C in 5% non-fat dry milk diluted in phosphate buffer saline (PBS) containing 0.05 % Tween 20. Membrane was incubated for 3h with primary antibody: anti-Twin Strep (1:1000) (BioRad), washed and subsequently incubated for 1h with secondary antibody: anti-mouse linked to peroxidase (Dako Agilent) (1:1000). The Clarity™ Western ECL substrate chemiluminescence kit (BioRad) and Amersham Imager 600 (GE Healthcare) were used for membrane visualization.

Chromatin immunoprecipitation followed by deep sequencing (ChIP-Seq)

ChIP-Seq assays were performed as described previously in [98]. Briefly, 80 ml of mid-log phase cells (OD_{660} of 0.6) were cross-linked in 1% formaldehyde and 10 mM sodium phosphate (pH 7.6) for 10 min at room temperature followed by 30 min on ice. Crosslinking was stopped by adding 125 mM glycine and incubation for 5 min on ice. Cells were washed three times in PBS, resuspended in 450 µl in TES buffer (10 mM Tris-HCl pH 7.5, 1 mM EDTA, 100 mM NaCl) and lysed with 2 µl of Ready-Lyse™ lysozyme solution (Epicentre) for 5 min at RT. Protease inhibitors (Roche) were added and incubated for 10 min. Then, 550 µl of ChIP buffer (1.1% triton X-100, 1.2 mM EDTA, 16.7 mM Tris-HCl pH 8.1, 167 mM NaCl, plus protease inhibitors) were added to the lysate and incubated at 37 °C for 10 min before sonication (2 x 8 bursts of 30 sec on ice using a Diagenode Bioruptor) to shear DNA fragments to an average length of 300-500 bp. Lysate was cleared by centrifugation for 10 min at 12,500 rpm at 4 °C and protein content was evaluated by measuring $OD_{280\ nm}$.Then, 7.5 mg of proteins were diluted in 1ml ChIP buffer supplemented with both 0.01% SDS and protease inhibitors; and incubated with 80 µl of MagStrep beads (Iba; Ref 2-4090-002) overnight at 4 °C with rotation. Beads were separated from the solution and washed once with low salt buffer (0.1% SDS, 1% Triton X-100, 2 mM EDTA, 20 mM Tris-HCl pH 8.1, 150 mM NaCl), once with high salt buffer (0.1% SDS, 1% Triton X-100, 2 mM EDTA, 20 mM Tris-HCl pH 8.1, 500 mM NaCl), once with LiCl buffer (0.25 M LiCl, 1% NP-40, 1% deoxycholate, 1 mM EDTA, 10 mM Tris-HCl pH 8.1), once with TE buffer (10 mM Tris-HCl pH 8.1, 1 mM EDTA) at 4 °C and a second wash with TE buffer at RT. The DNA-protein complexes were eluted twice in 250 µl of Biotin Elution Buffer BX (Iba; Ref 2-1040-050). Both eluates were combined (500 µl) and NaCl was added to a final concentration of 250 mM before overnight incubation at 65 °C to reverse the crosslink. The samples were treated with 20 µg of proteinase K in 40 mM EDTA and 40 mM Tris- HCl (pH 6.5) for 2 h at 45 °C. DNA was extracted using Nucleospin PCR clean-up kit (Macherey-Nagel) and resuspended in prewarmed 50 µl elution buffer (5 mM Tris-HCl pH 8.5). DNA sequencing was performed by BIO, part of the IPG (Institut de Pathologie et de Génétique).

Sequencing data analysis

Sequencing reads were mapped with BWA[99] against *C. crescentus* NA1000 reference genome (NC_0119160.1) and filtered using SAM tools[100]. Model based analysis of ChIP-seq (MACS)[101] was used to estimate DNA fragment size as well as shift size. Next, the number of reads overlapping each genomic position was computed using custom Python scripts together with the previously modelled DNA fragment and shift sizes. A peak was defined as the genomic region where each position has more reads than the 97th percentile.

Protein alignments

The blastp algorithm was used to search for homologous proteins in *C. crescentus* NA1000 (taxid:565050). EMBOSS Needle was used for pairwise sequence alignments. Scores and percentages in identity, similarity and gaps were calculated with the EBLOSUM62 matrix, a gap penalty of 10.0 and an extend penalty of 0.5.

Statistical analysis

Analyses were performed using the GraphPad Prism 8 software. The significance of differences between mean values was determined by bilateral t-test, one-way or two-way ANOVAs followed by a Tukey's test for multiple comparisons. Annotations respectively refer to the NEJM *p*-values; 0.12 (ns), 0.033 (*), 0.002 (**) and <0.001 (***).

1 K^+ is an essential environmental cue for cell cycle progression in *C. crescentus*

To primarily assess the impact of K^+ on fitness, *C. crescentus* wild-type strain was grown in K_0 minimal media supplemented with different K^+ concentrations. Low K^+ conditions (0.025 mM K^+) induced a strong growth defect compared to higher K^+ conditions (0.5 mM K^+) (Fig. 7A). Importantly, *C. crescentus* failed to grow in unsupplemented K_0 media, from now on referred to as K^+-depleted conditions (Fig. 7A). The strict requirement of K^+ supplementation for growth confirms the significance of this ion, as it has been reported in other bacteria.

Since Rb^+ and Cs^+ are known to fulfil certain K^+-related functions due to their similar properties, we aimed to test if some alkali metals could restore the growth defect observed in low K^+ conditions. To that end, low K^+ conditions were supplemented with 0.5 mM of Li^+ (lithium), Na^+ (sodium), Rb^+ or Cs^+. While the addition of Cs^+ surprisingly slowed down growth, neither Li^+ nor Na^+ had an impact (Fig. 7B, supplementary Fig. 1A and 1B). In contrast, Rb^+ could partially restore growth; the doubling time was consequently decreased (Fig. 7B, supplementary Fig. 1A and 1B). This suggests that Rb^+ can substitute, at least partially, K^+ in some functions contributing to fitness.

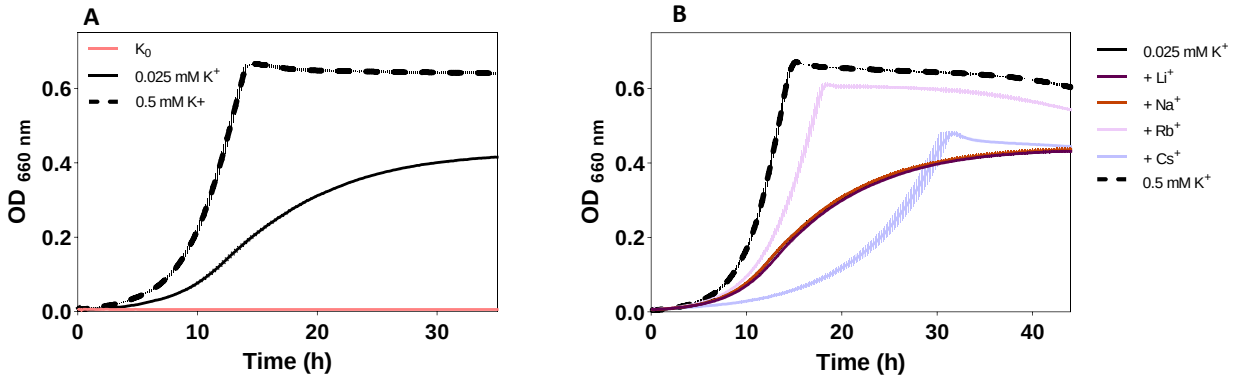

Figure 7. Impact of environmental K^+ conditions on *C. crescentus.*
C. crescentus was grown in depleted (K_0), low 0.025 mM K^+ and high K^+ conditions (0.5 mM K^+) (A). Rb^+ can partially restore the growth defect observed in low K^+ (B). Alkali metals were added to low K^+ conditions at a concentration of 0.5 mM. Error bars= ±SD; n=3

To further investigate if K^+ is required for cell cycle progression, the DNA content of a synchronized population was followed throughout growth in depleted, low and high K^+ conditions (Fig. 8A-C). After synchrony (T_0), nearly all cells in the population are swarmers (G1). Cell division rapidly occurred over time in low and high K^+ conditions, the majority of cells reached S and G2 phase after one and two hours of growth, respectively (Fig. 8B-C). In contrast, cells grown in K^+-depleted conditions accumulated in G1 phase (Fig. 8A). Around 94 % of cells were still in G1 phase at T_{60} against 43,93 % and 30,80 % for low and high K^+, respectively (Fig. 8D). At T_{120}, the proportion of cells in G1 barely decreased to 86.56 %, compared to 12.23 % and 21.30% for low and high K^+, respectively (Fig. 8D). Although low K^+ leads to a growth defect, supplementation of the media with 0.025 mM K^+ seems sufficient to allow cell division within the first hours of growth at least.

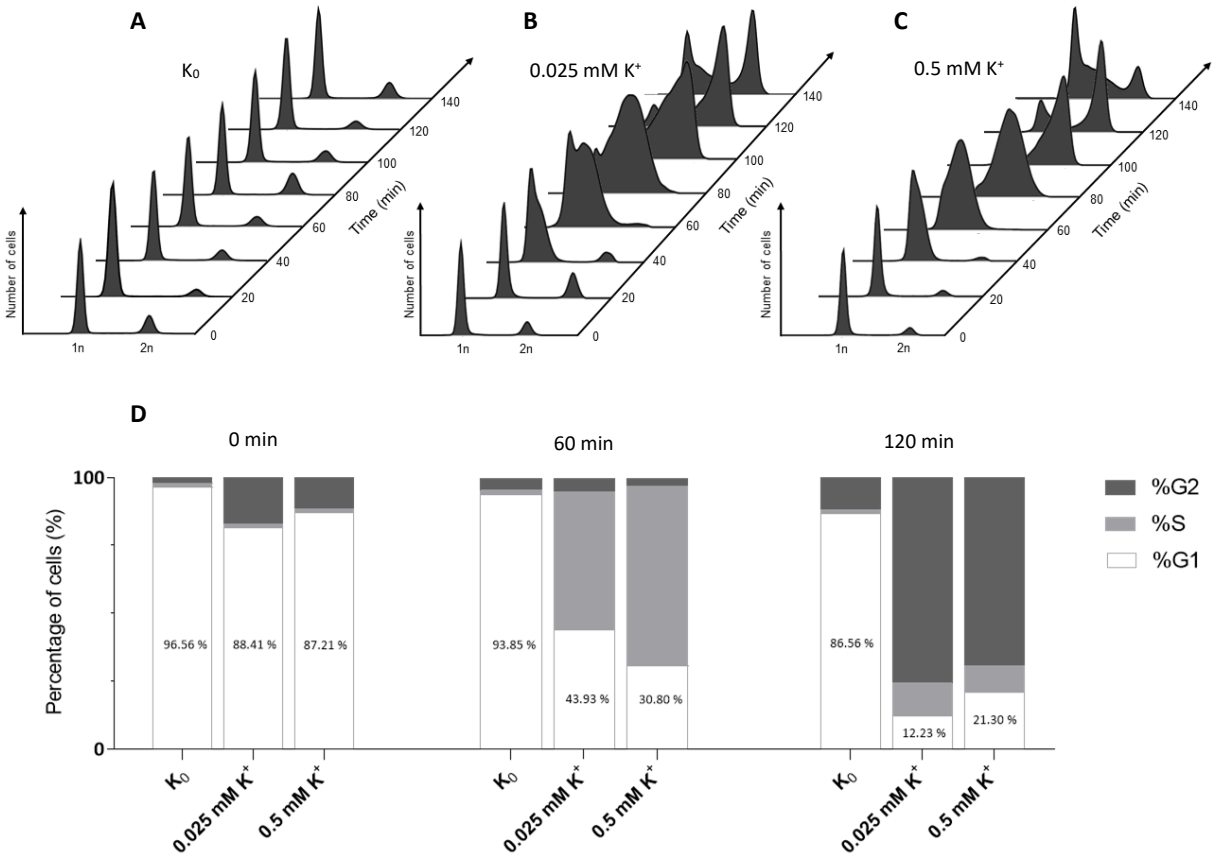

Figure 8. *Caulobacter crescentus* accumulates G1/swarmer cells upon K^+ depletion.
Flow cytometry analysis was used to determine DNA content throughout the cell cycle of a synchronized population of wild-type strain grown in K_0 (A), 0.025 mM K^+ (B) and 0.5 mM K^+ (C). Samples were withdrawn every 20 minutes for 140 minutes. Proportions of cells in G1, S and G2 phases at T_0, T_{60} and T_{120} (D). Analysis was performed using the BD FACSuite V1.0.5 software (D).

These results show that swarmer cells cannot initiate DNA replication in K^+-depleted conditions, suggesting that K^+ is essential for cell cycle progression in *C. crescentus*. This highlights K^+ depletion as another stressful condition leading to an extension of the G1/swarmer phase.

To gain some insights on this regulation, both cytoplasmic and periplasmic K^+ concentrations were measured with the aim of determining whether they were influenced by environmental K^+ conditions. Cells were grown to exponential phase in low and high K^+ conditions prior to fixation and cell fractionation. Both cytoplasmic and periplasmic K^+ concentrations showed no significant difference between cells grown in low or high K^+ (Fig. 9). In each condition, cytoplasmic concentrations were close to 100 mM while periplasmic concentrations ranged from 650 to 750 mM. This finding suggests that *C. crescentus* maintains steady intracellular K^+ levels regardless of environmental conditions. On one hand, this implies that cells grown in high K^+ conditions do not necessarily tend to accumulate more K^+ than apparently required, although it is available. On the other hand, the maintenance of steady K^+ intracellular levels even in low K^+ hints towards an ability to adapt to these conditions.

Since the Kdp transport system is predicted to be expressed and active in low K^+, it is likely involved in the maintenance of K^+ homeostasis in those conditions. This work will therefore be focused on characterizing the *kdpABCDE* operon in *C. crescentus* and on investigating if this system contributes to the K^+-dependent cell cycle regulation.

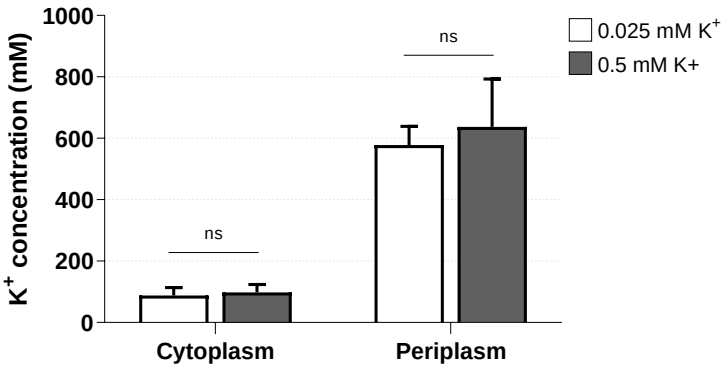

Figure 9. Cytoplasmic and periplasmic K^+ concentrations are not impacted by environmental K^+ conditions.

Cells were grown in 30 ml of K_0 media supplemented with 0.025 mM K^+ or 0.5 mM K^+ until mid-exponential phase prior fixation and cellular fractionation. K^+ concentrations were determined by ICP-OES.

Statistical analysis was carried out via a bilateral student test ($P > 0.05$). Error bars= ±SD; n=3.

2 *In silico* analysis of the *kdpABCDE* operon

Since the *E. coli* Kdp proteins are the best characterized, their sequences were used as input to conduct BlastP searches in *C. crescentus* (Table 1). Putative homologs of all Kdp proteins were identified in *C. crescentus*, except KdpF for which there were no significant hits. Unlike the genetic organization in *E. coli*, all Kdp proteins are encoded in a single operon (*kdpABCDE* operon).

Putative Kdp homologs were subjected to pairwise alignments to the *E. coli* sequences in order to determine the percentages of identity, similarity and gaps. All alignments resulted in identity values greater than 35 %, supporting their homology [102]. Among them, the P-type ATPase KdpB exhibited the highest value in both identity (59.0 %) and similarity (72.6 %). In contrast, the HK KdpD yielded the lowest percentage of identity (36.3 %). Comparison of Kdp sequences with other α-proteobacteria generated higher values in both identity and similarity for all proteins. Although still displaying the lowest identity value, *C. crescentus* KdpD sequence was identical at 42.8 %, 43.0 % and 45.5 % respectively with that of *Rhizobium leguminosarum*, *Agrobacterium tumefaciens* and *Sinorhizobium meliloti.*

Table 1. Protein blasts searches in *C. crescentus* using *E. coli* Kdp sequences as input. Percentages in identity, similarity and gaps were determined using EMBOSS Needle with EBLOSUM62 as a matrix, a gap penalty of 10.0 and an extend penalty of 0.5.

INPUT	HIT	SCORE	E-VALUE	PAIRWISE ALIGNEMENT		
				IDENTITY	SIMILARITY	GAPS
KdpF	No significant hit	/	/	/	/	/
KdpA	CCNA_01663-MONOMER Potassium-transporting ATPase A chain	448	1,00E-151	46.4 %	63.6 %	2.6 %
KdpB	CCNA_01664-MONOMER Potassium-transporting ATPase B chain	776	0	59.0 %	72.6 %	4.6 %
KdpC	CCNA_01665-MONOMER Potassium-transporting ATPase C chain	152	1,00E-46	46.0 %	57.0 %	6.5 %
KdpD	CCNA_01666-MONOMER Osmosensitive K+ channel histidine kinase kdpD	481	1,00E-155	36.3 %	53.0 %	4.8 %
KdpE	CCNA_01667-MONOMER Two-component response regulator kdpE	203	2,00E-65	44.4 %	61.6 %	3.0 %

Kdp protein sequences were further analysed by identifying domains and their organization (Fig. 10). Comparison of Pfam features highlighted that the KdpD sequence of *C. crescentus* lacks the cytoplasmic GAF domain known to be linked to the DHp domain in *E. coli* [103]. Multiple sequence alignments enabled to locate the conserved catalytic histidine (His670) and aspartate (Asp56) residues of the KdpD HK and the KdpE RR, respectively (Fig. 10A and 10B). On top of this, the four conserved residues presumably involved in periplasmic K^+ sensing by KdpD were also identified: Phe461, Ser466, Phe467 and Val469 (Fig. 10A).

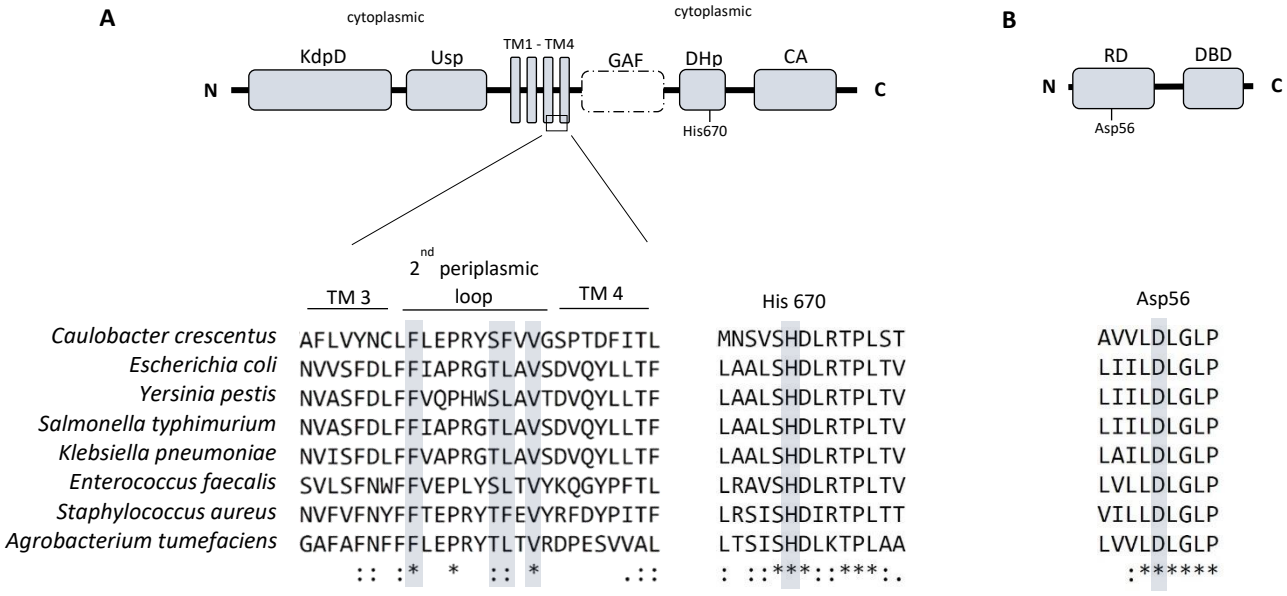

Figure 10. Domain architectures and relevant conserved residues in *C. crescentus* KdpD (A) and KdpE (B).
Protein domains were predicted by searching the Pfam database (cut-off E value = 1.0). Accession numbers are as follows: KdpD (PF02702), Usp (PF00582), Dhp (PF00512), CA (PF02518), RD (PF00072) and DBD (PF00486). Multiple sequences alignments were performed with Clustal Omega. KdpD protein sequences were as follows: *C. crescentus*, Uniprot: A0A0H3C8H5; *E. coli*, UniProt: P21865; *Y. pestis*, UniProt: Q7CJR5; *S. typhimurium*, UniProt: Q8ZQW4; *K. pneumoniae*, UniProt: B5XZF1; *E. faecalis*, UniProt: Q838F4; *S. aureus*, UniProt: A0A0H2XIE2; and *A. tumefaciens*, Uniprot: A0A2L2LHM9. KdpE proteins sequences were as follows: *C. crescentus*, Uniprot: A0A0H3C8M3; *E. coli*, UniProt: P21866; *Y. pestis*, UniProt: Q0WDK2; *S. typhimurium*, UniProt: Q8ZQW5; *K. pneumoniae*, UniProt: A0A0W8ASI2; *E. faecalis*, UniProt: J5B8M5; and *S. aureus*, UniProt: Q2FWH6; and *A. tumefaciens*, Uniprot: A0A1B9TGM5.

3 Kdp system

As expected, deletion of the Kdp transport system impaired growth exclusively in low K^+ conditions (Fig. 11A). The triple knockout mutant, Δ*kdpABC,* showed an increased doubling time compared to the wild-type strain in low K^+ (Fig. 11B). In contrast, doubling times are not significantly different in high K^+ (Fig. 11B). The growth defect of Δ*kdpABC* could also be observed on K_0 plates (Fig. 11C). Since no growth was detected for the wild-type strain in K_0 liquid media (Fig. 7A), it is very likely that residual amount of K^+ is provided by the agar on K_0 plates.

In order to study the Kdp system at the transcriptional level, a plasmid carrying a P_{kdp}::*lacZ* reporter fusion was introduced in both wild-type and Δ*kdpABC* strains. Cells were grown overnight in low and high K^+ and β-galactosidase activity was measured. For both strains, expression of the P_{kdp}::*lacZ* fusion was weak in high K^+, while drastically increased in low K^+ (Fig. 11D). Together, these data support that the Kdp system mainly contributes to K^+ uptake in low K^+ conditions.

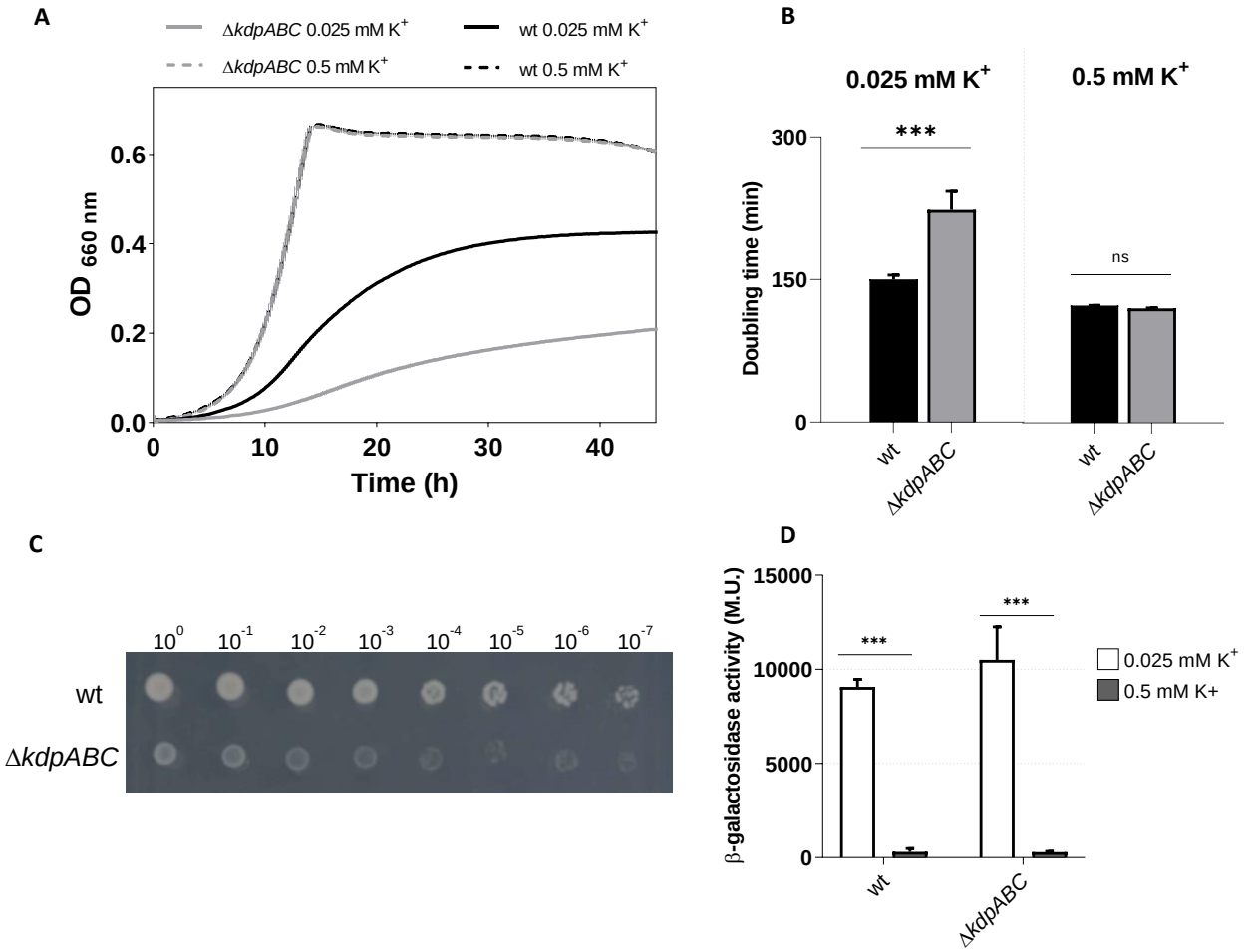

Figure 11. The Kdp system mainly contributes to K^+ uptake in low K^+ conditions.
Wild-type and Δ*kdpABC* strains grown in low K^+ (dotted line) and high K^+ (plain line) (A) and their respective doubling time (B). Serial dilutions spotted on K_0 plates (1 % agar) (C). β-Galactosidase activities of wild-type and Δ*kdpABC* strains carrying a transcriptional P_{kdp}::*lacZ* fusion grown in low and high K^+ (D). Statistical analyses were carried out via two-ways ANOVA followed by Tukey's test for multiple comparisons. Error bars= ±SD; n=3.

4 The KdpD/E two-component system works in a different fashion than in *E. coli*

The last two genes of the *kdp* operon in *C. crescentus* respectively encode the HK KdpD and the RR KdpE, forming together a two-component system presumably involved in the regulation of K^+ uptake through transcriptional activation.

Surprisingly, deletion of *kdpD* generated phenotypes inconsistent with what had been previously reported. In *E. coli*, *kdp* is not expressed in a Δ*kdpD* mutant and the latter does not survive in K^+ limitation unless it acquires suppressor mutations [74]. In low K^+ conditions, Δ*kdpD* displayed a slower growth than the wild type but reached a higher final OD (Fig. 12A-C). To test for complementation, a low-copy plasmid carrying a P_{kdp}::*kdpD* fusion was introduced in Δ*kdpD.* A wild-type growth pattern was partially restored in the complemented strain (Fig. 13A-C). Although the doubling time of the complemented strain was slightly higher than the one of the wild-type strain carrying an empty plasmid (Fig. 13A and Fig. 13B), both reached the same final OD (Fig. 13A and Fig. 13C).

The catalytically inactive mutant (*kdpD*$_{H670N}$) showed similar features than that of Δ*kdpD* (Fig. 12A-C). More importantly, β-galactosidase assays demonstrated that the *kdp* operon was expressed even in the absence of the sensor kinase (Fig. 12D). Since the gene product of *lacZ* accumulates along growth, measurements of β-galactosidase activities in overnight cultures provide little information about the kinetics of promoter activation. We therefore followed the expression of the P$_{kdp}$::*lacZ* fusion in both wild-type and *kdpD*$_{H670N}$ strains carrying the reporter plasmid throughout growth in low K$^+$ conditions. Compared to the wild-type strain, *kdpD*$_{H670N}$ displayed lower β-galactosidase activities within the 20 first hours of growth (Fig. 12E). Expression of the P$_{kdp}$::*lacZ* fusion was significantly increased when the growth of *kdpD*$_{H670N}$ surpassed that of the wild-type (Fig. 12E). These results demonstrate that the *kdp* operon of *C. crescentus* can be expressed without activation of the HK and that the latter seems to act as negative regulator of the response to K$^+$ limitation.

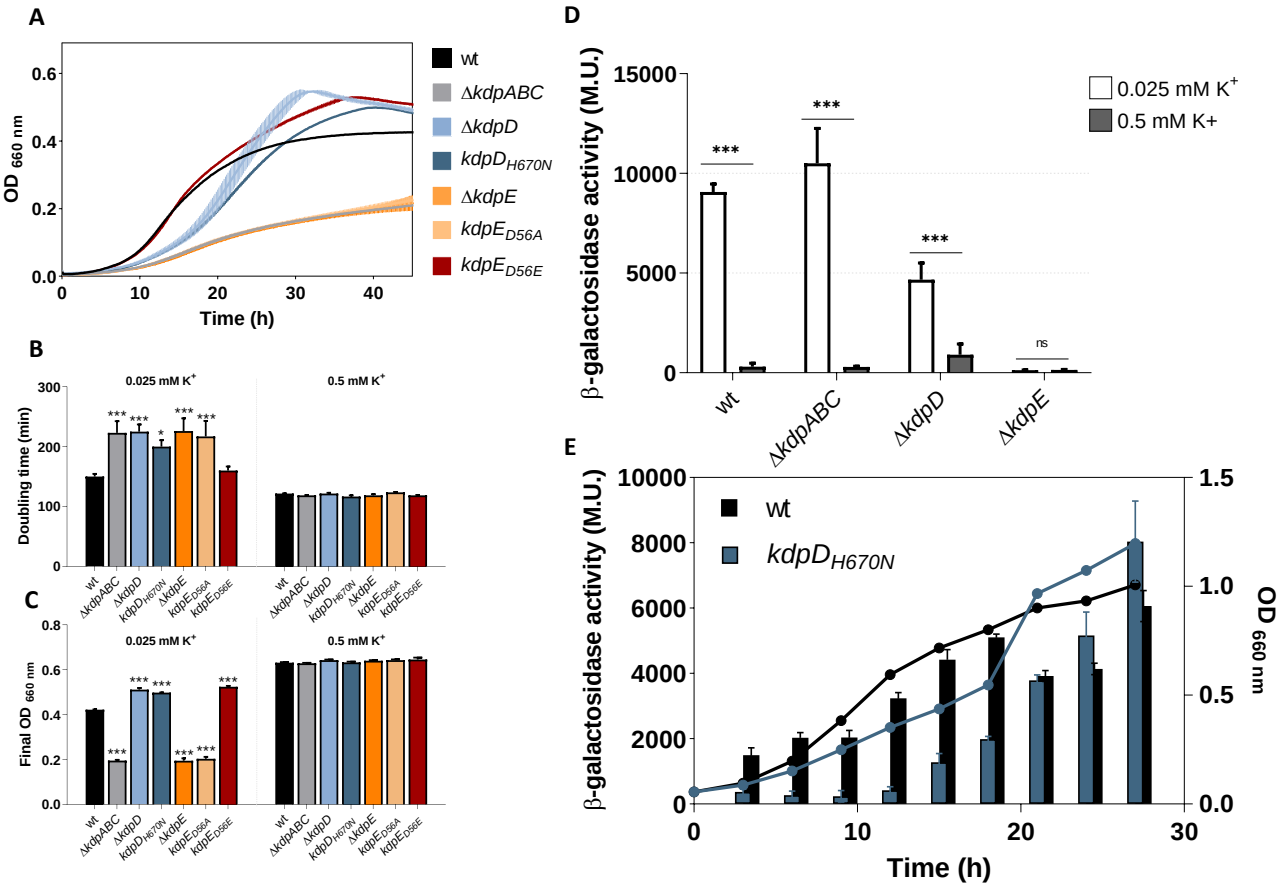

Figure 12. Mutations in *kdpDE* reveal negative regulatory roles in the response to K$^+$ limitation.
Growth curves of indicated strains in low K$^+$ conditions (A). Their doubling time (B) and final ODs (C) in low and high K$^+$ conditions. β-Galactosidase activities of wild-type and Δ*kdpABC*, Δ*kdpD* and Δ*kdpE* strains carrying a transcriptional P$_{kdp}$::*lacZ* fusion grown in low and high K$^+$ (D). Comparison of β-Galactosidase activities in wild-type and *kdp*$_{H670N}$ strains along growth in low K$^+$ conditions. Statistical analyses were carried out via two-ways ANOVA followed by Tukey's test for multiple comparisons. Error bars= ±SD; n=3.

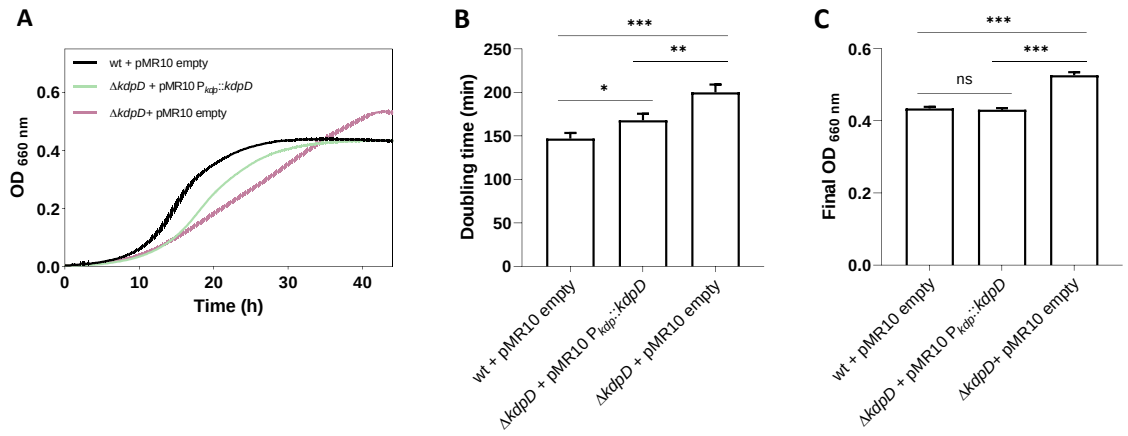

Figure 13. Complementation of Δ*kdpD* partially restores the wild-type phenotype.
Growth curves of both wild-type and Δ*kdpD* carrying an empty plasmid and Δ*kdpD* complemented strain in low K^+ conditions (A), their respective doubling time (B) and final ODs (C). Statistical analyses were carried out via one-way ANOVA followed by Tukey's test for multiple comparisons. Error bars= ±SD; n=3.

To investigate the cell cycle progression in Δ*kdpD*, the DNA content of a synchronized population was followed throughout growth in low K^+ conditions. Compared to the wild-type strain, Δ*kdpD* accumulated more cells in G1 phase (Fig. 14A and 14B). At T_{40}, around a quarter of the wild-type population entered S phase while the percentage of cells in S phase almost remained unchanged in Δ*kdpD* (Fig. 14C). At T_{80} and T_{120}, the proportion of cells in G1 phase is around twice as high in Δ*kdpD* as in the wild-type strain (Fig. 14C). These data indicate that Δ*kdpD* cells spend more time in G1 phase likely to reach a critical K^+ intracellular concentration, which explains the slower growth rate of Δ*kdpD* in low K^+ conditions.

In the absence of the RR KdpE, growth in low K^+ conditions was similar to that of Δ*kdpABC.* Substitution of the catalytic aspartate by alanine ($kdpE_{D56A}$), resulting in a phospho-inactive mutant, induced the same phenotype. In contrast, the phospho-mimetic mutant, $kdpE_{D56E}$, displayed a doubling time similar to the wild type and even reached a higher final OD. This suggests that, as in *E. coli*, KdpE controls the expression of the transport system at the transcriptional level. Consistent with this idea, β-galactosidase activity was drastically reduced in both Δ*kdpE* and $kdpE_{D56A}$ grown in low K^+ conditions (Fig. 12D and supplementary Fig.2).

To characterize the KdpE regulon, we performed chromatin immunoprecipitation followed by deep sequencing (ChIP-seq). A tagged version of *kdpE* was integrated under the chromosomal xylose-inducible promoter P_{xylX} in Δ*kdpE.* Expression of the protein fusion in Δ*kdpE* - $P_{xylX::}$*kdpE-tag* was verified by western blot in presence of xylose (Fig. 15A) and the functionality of the tagged protein was also confirmed (Fig. 15B). ChIP-seq experiments were performed in both low and high K^+ conditions. Analyses of sequencing reads could not highlight any significant peak in either of the two conditions. It seems unlikely that KdpE-regulated promoters are inexistant but rather that the ChIP-seq experiment itself was not optimal. Although Δ*kdpE* P_{xylX}*::kdpE-tag* showed a significantly decreased doubling time compared to Δ*kdpE*, the difference is not striking. The presence of xylose for induction reduces disparities in growth and the limit between non-functional and functional protein becomes quite thin. Measurements of the P_{kdp}::*lacZ* expression would probably have been a more appropriate experiment to check the functionality of the tagged KdpE but new constructions would have been required since both plasmid have the same antibiotic resistance. Meanwhile, the *C. crescentus* KdpE had been purified (Supplementary Fig. 3) to immunize rabbit for polyclonal antibodies production. After assessment of their specificity, α-KdpE will be used to repeat ChIP-seq in a wild-type background in both low and high K^+ conditions.

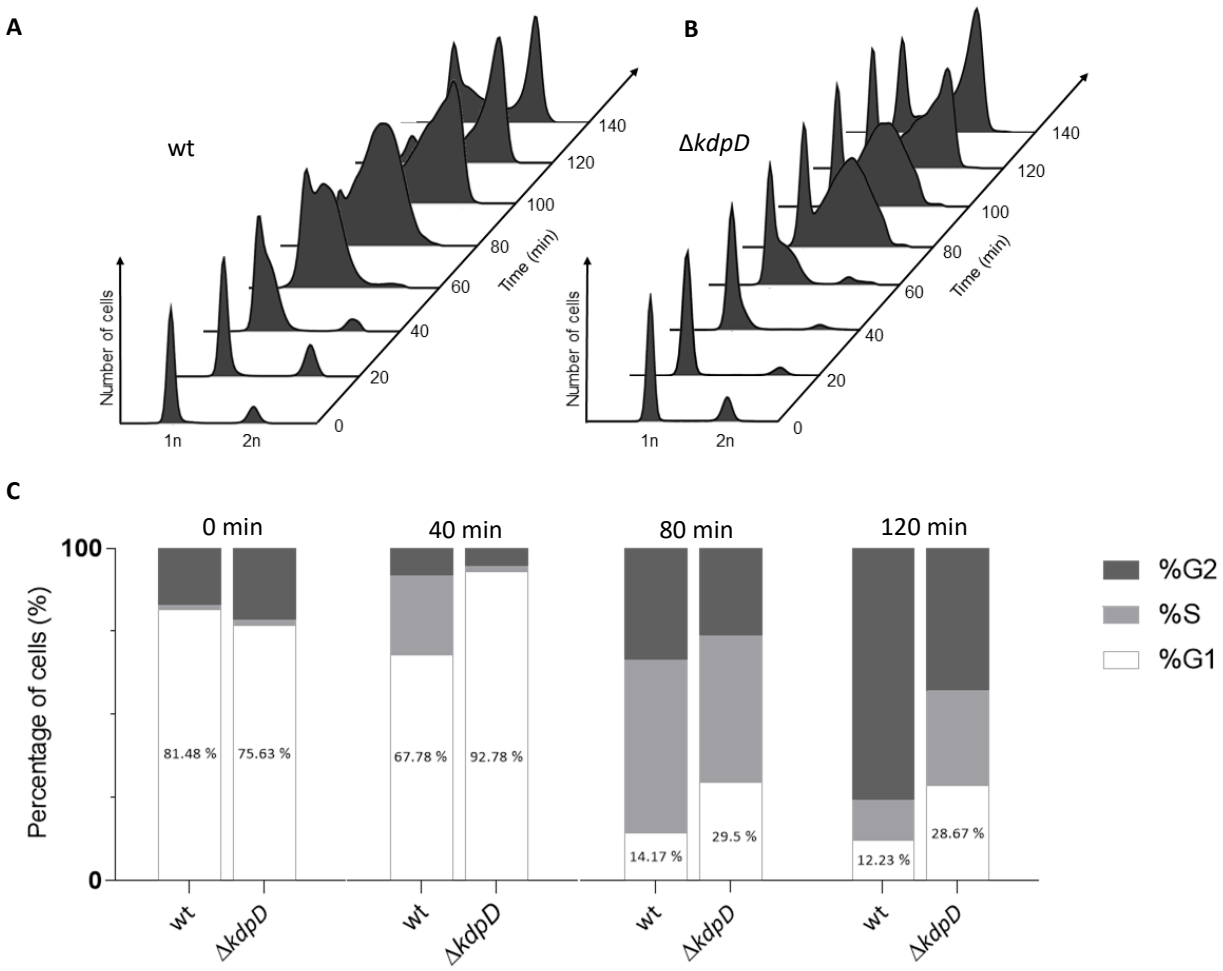

Figure 14. The Δ*kdpD* mutant displays a G1 accumulation in low K^+ conditions.
Flow cytometry analysis was used to determine DNA content throughout the cell cycle of synchronized populations of wild-type (A) and Δ*kdpD* (B) strains grown in low K^+ conditions. Samples were withdrawn every 20 minutes for 140 minutes. Proportions of cells in G1, S and G2 phases at T_0, T_{40}, T_{80} and T_{120} (C). Analysis was performed using the BD FACSuite V1.0.5 software.

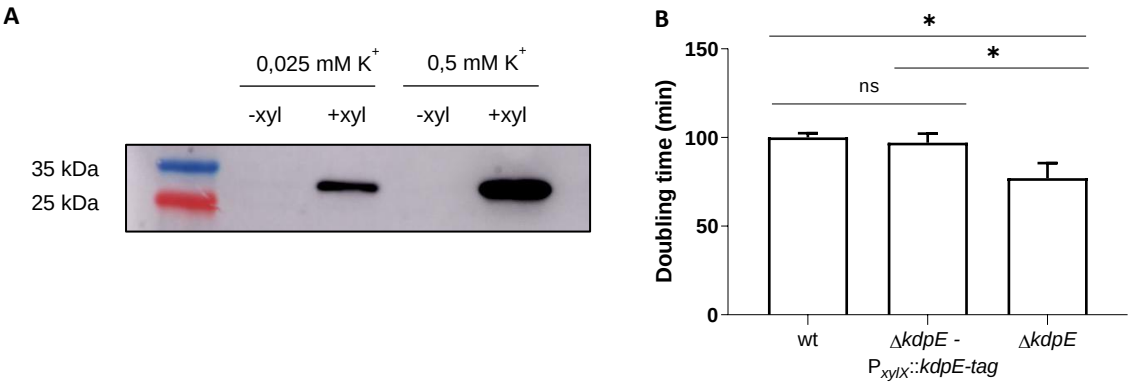

Figure 15. Detection (A) and functionality (B) of tagged-KdpE. Statistical analyses were carried out via one-way ANOVA followed by Tukey's test for multiple comparisons. Error bars= ±SD; n=3

K^+ is essential for living cells because it is involved in multiple cellular processes including osmoregulation, membrane potential maintenance, pH regulation, translation, protein folding, *etc* (reviewed in [2]). It is especially crucial for the activity of the ribosome and several key enzymes such as the translation factor EF-Tu [5], the pyruvate kinase [8] or chaperonin GroEL [7]. As demonstrated in other organisms [22,42], the absence of *C. crescentus* growth in K^+-depleted conditions emphasizes the requirement for K^+ (Fig. 7A).

Our data showed that Rb^+ can partially compensate for the lack of K^+ in low K^+ conditions (Fig. 7B, supplementary Fig. 1A and 1B). Due to their similar features, Rb^+ is known to be transported through the same paths as K^+ [2], i.e. Kdp, Trk and Kup in *E. coli*. On account of that, $^{86}Rb^+$ was long used as a radioactive tracer for K^+ transport [104]. With the aim of assessing the accuracy of this tracer, the ability of Rb^+ to satisfy the cell's requirement for K^+ was determined in *E. coli*. This study showed that Rb^+ could stimulate growth but at much higher concentrations than K^+, suggesting that Rb^+ can perform K^+-related functions but with less effectiveness. Also, despite the presence of Rb^+, cells required a minimum amount of K^+, presumably for the activation of cellular enzymes [1,104]. It was recently shown in *Bacillus subtilis* that the lack of K^+ could also be compensated by the addition of positively charged amino acids proposed to take over the neutralizing function of K^+ [22].

1 K^+-dependent cell cycle regulation

We have shown in this work that *C. crescentus* extends its G1/swarmer phase upon K^+ depletion. *C. crescentus* responds likewise to other stress conditions, such as carbon and nitrogen depletion [89,90]. Although active and energy consuming, the motile morphotype is ideal to explore and increase chances of finding new suitable environments [105,106]. The mechanisms of the nitrogen-dependent response have been lately studied in detail [89]. Here we have shown that the low affinity Kdp system is important to guarantee a cell cycle progression in K^+-depleted conditions. Nonetheless, our experiments also show that although Kdp is important, it is not essential in *C. crescentus*. The definite mechanisms behind this response to K^+ depletion remain an open question. Here, below, several regulatory mechanisms related to cell cycle and environmental stress response are discussed.

1.1 K^+-dependent processes inherent to cell cycle progression

Previous studies have shown that intracellular K^+ levels fluctuate according to K^+ conditions in the environment [22,51,59]. In contrast, our results suggest that, in *C. crescentus,* K^+ concentrations are steady under different K^+ environmental regimes (Fig. 8). However, in this work, a long period of adaptation preceded K^+ concentrations measurements. Cells were indeed grown in low and high K^+ conditions overnight to reach exponential phase the next day before proceeding to fixation and cellular fractionation. It is possible that concentrations measured thereafter reflect a timing where bacteria had already reinstated homeostasis. To test this possibility, intracellular K^+ concentrations could instead be monitored kinetically throughout growth after the transfer of cells from high to low K^+ conditions[5]. Additionally, other methods than ICP-OES could be used to further test whether the intracellular K^+ conditions remain intact in different environments. For instance, fluorescent reporters for intra- and extracellular K^+ concentrations, respectively thioflavin (ThT) and asante potassium green-4 (APG-4), could help to define the ion flux dynamics[19].

Besides being required by numerous enzymes related to basic metabolic functions [2,107], K^+ modulates the activity of several cell cycle enzymes in multiple bacteria. For instance, in *E. coli*, K^+ has been shown to stimulate the polymerizing activity of DNA polymerase [108]. The rate at which nucleotides are incorporated *in vitro* increased with K^+ concentrations [108]. Additionally, K^+ ions were reported as essential for the DNA supercoiling activity of DNA gyrase in both *B. subtilis* [109] and *Micrococcus luteus* [110]. This enzyme removes DNA knots that agglomerate in front of replication forks and transcription complexes [111]. It does so by introducing negative supercoils in an ATP-dependent manner [111]. In *B. subtilis*, DNA supercoiling activity was reported exclusively in presence of K^+ and not in the presence of Na^+. While K^+ only mildly affected both ATP binding and hydrolysis, it is suggested to stabilize the ATPase domain thereby allowing conformational change associated with strand passage at the protein-DNA interface [109,112].

Aside from modulating enzymatic activities, K^+ was shown to influence the polymerization of FtsZ, key component of the bacterial cell division machinery [113,114]. This tubulin-like GTPase polymerizes in a GTP-dependent manner to form protofilaments that assemble with each other as a ring (Z-ring) at midcell. Formation of the dynamic Z-ring requires both assembly and disassembly of these FtsZ polymers. At physiological pH, the binding of K^+ to FtsZ was reported essential for polymerization in *E. coli* [114]. Additionally, the length of the protofilaments was shown to be reduced in low K^+ conditions [113]. Authors suggested that the K^+-dependent modulation of protofilaments length would be related to the subunit turnover rate of rather than a modulation of the GTPase activity as previously proposed. Regardless of the exact mechanism, the influence of K^+ on dynamics of FtsZ protofilaments provides a possible explanation for its regulation over cell cycle.

K^+ is also a key regulator of membrane potential, which is considered as an important bioelectric parameter influencing cell cycle progression. For instance, in ovary cells, DNA synthesis is completely blocked when the membrane potential is forced to a fixed hyperpolarized value [31]. In bacteria, a study reported that membrane potential modulates the localization of proteins involved in cell division [115]. Not much is known about the relationship between K^+ and membrane potential in bacteria. However, recent studies [19,20] have characterized an electrical signalling in bacterial communities that is based on K^+-mediated fluctuations in membrane potential. In *B. subtilis*, an increase in extracellular K^+ was shown to trigger a depolarization of cells. This supports that environmental K^+ conditions induce fluctuations in membrane potential that could accordingly alter cell cycle progression.

Importantly, changes in membrane potential mediated by K^+ were reported to influence motility: free motile cells are attracted by extracellular K^+. This chemotactic response to K^+ has been demonstrated in both *B. subtilis* and *P. aeruginosa*, suggesting that it also applies to a large number of bacterial species. The proposed mechanism behind this electrical attraction is the following: when cells encounter high extracellular K^+ conditions, they undergo a depolarization that is in response immediately followed by a hyperpolarization of cells. As a result, the proton motive force (PMF) is increased, and the tumbling frequency of motile cells is reduced. The cell therefore continues to swim in the same direction and towards the increasing K^+ gradient. The chemoattractant nature of K^+ is consistent with the extension of the swarmer phase upon K^+-depletion. When K^+ is limiting, *C. crescentus* extends the lifetime of the chemotactically active swarmer cell, thereby promoting spreading and colonization of environments enriched in K^+ to pursue cell differentiation and division.

Measuring membrane potential values in different K^+ conditions could assess if membrane potential contributes to the K^+-dependent cell cycle regulation in *C. crescentus.* The carbocyanine dye $DiOC_2(3)$ is commonly used to detect membrane potential: its fluorescence shifts from green to red with larger membrane potentials and the calculated ratio of fluorescence intensity can be compared between test conditions [116]. It is also worth investigating the chemotactic response to K^+ in *C. crescentus* through microfluidics and speed measurements at the single cell level.

1.2 K^+-dependent sigma factor selectivity

Intracellular K^+ levels are known to influence the competition between sigma factors for interaction with the RNAP *in vivo*. In *E. coli,* elevated K^+ conditions (500 mM K^+-glutamate) preferentially promote complex formation between RNAP and σ^S rather than σ^{70}. By affecting sigma factor selectivity, K^+ intracellular levels can easily direct the RNAP towards σ^S -dependent stress response genes and activate their expression.

Most organisms rely on tightly controlled programs of gene expression for cell cycle progression. For instance, in *C. crescentus*, the alternative sigma factor σ^{54} (*rpoN*) greatly contributes to morphogenesis and cell differentiation [117,118]. It is essential for the biogenesis of both flagellum and stalk and these developmental events are subjected to a tight regulation. First, *rpoN* is only temporarily expressed during the cell cycle and second, the transcription of specific σ^{54}-dependent genes, such as flagellar genes, additionally requires different transcriptional activators [118].

Although the function of all the 17 sigma factors in *C. crescentus* has yet to be identified, K^+-dependent sigma factor selectivity may play a role in cell cycle progression by adding another level of regulation for the transcription of cell cycle related genes. As described in [77], a large set of assays can demonstrate such regulation. First, expression levels of a σ^x-dependent gene may be compared in different K^+ conditions via β-galactosidase assays. Furthermore, pull down assays followed by mass spectrometry identification can enable to determine which σ factors are bound to RNAP when *Caulobacter* cells are grown in different K^+ conditions. Once identified, the force of the interaction between RNAP and σ^x could be determined *in vitro* by using for instance surface plasmon resonance.

1.3 Second messengers

Cyclic nucleotides

As demonstrated in several Gram-positive bacteria, K^+ homeostasis is massively regulated by c-di-AMP [51,81–84]. When synthesized, this second messenger negatively regulates both activity and expression of K^+ transport system. Upon K^+ limitation, c-di-AMP levels are decreased, and its repression is lifted. Although this second messenger is not synthesized in α-proteobacteria, *C. crescentus* produces its sibling cyclic nucleotide, c-di-GMP, whose regulatory networks have been extensively studied. It has been identified as an important regulator of cell cycle. It is particularly responsible for the swarmer to stalked differentiation and this transition is correlated with a peak in c-di-GMP levels.

If we speculate that c-di-GMP levels fluctuate reminiscently to that of c-di-AMP, K^+-depletion would result in low c-di-GMP levels thereby preventing progression in cell cycle. It remains unclear how K^+ limitation leads to a decrease in c-di-AMP levels but the enzymes producing c-di-AMP in *B. subtilis* were less abundant in low K^+ conditions[51]. Measuring intracellular c-di-GMP levels by mass spectrometry could assess if such regulation occurs.

Supporting a link between c-di-GMP and K^+, a c-di-GMP binding protein called DgrA, is encoded adjacent to the *kdp* operon. Consistent with the c-di-GMP dependent swarmer to stalked transition, DgrA blocks motility by interfering with the flagellar motor function [119].

(p)ppGpp

Besides K^+, deprivation of other nutrients like nitrogen and carbon also induces an extension of the G1/swarmer phase. Such nutritional stresses have been linked to the accumulation of an alarmone known as (p)ppGpp, the guanosine tetra- and penta- phosphate. Studies have demonstrated that the accumulation (p)ppGpp, triggered upon nitrogen and carbon starvation, was responsible for the extension of the swarmer phase in those conditions. At the core of the stringent response, the synthesis of (p)ppGpp mediates a rapid and massive switch in the allocation of cellular resources through a large array of mechanisms [93]. Accordingly, this alarmone modulates a wide range of cellular processes including cell cycle progression [120,121]. In *B. subtilis*, the presence of (p)ppGpp inhibits elongation of DNA replication within minutes [121]. Progression of the replication fork is arrested by the direct binding of (p)ppGpp to the DNA primase, a crucial component of the replication machinery. In *C. crescentus*, (p)ppGpp was shown to simultaneously delay the swarmer-to-stalked differentiation and G1 to S transition by modulating transcriptional profile. Indeed, (p)ppGpp binds directly to the RNAP (J. Coppine, unpublished data) and likely influence the affinity between RNAP and sigma factors in a similar way than the one described in *E. coli* [93,122].

An accumulation of (p)ppGpp upon K^+ depletion could therefore explain the resulting extension of the swarmer phase. Supporting this idea, the regulatory network connecting nitrogen starvation to (p)ppGpp accumulation in *C. crescentus* involves PTS^{Ntr} (See section 4 of introduction) [89], which has been previously associated with K^+ homeostasis in other bacteria [74,123]. In this network, EI^{Ntr} detects nitrogen starvation by sensing intracellular glutamine levels thanks to a GAF domain. Glutamine deprivation therefore promotes the phosphorylation of EI^{Ntr} and downstream PTS^{Ntr} components in *C. crescentus*: HPr and $EIIA^{Ntr}$. The latter two were shown to modulate SpoT enzymatic activities, thus triggering (p)ppGpp accumulation which consequently delays cell cycle progression.

Additionally, a mechanism of regulation connecting K^+ homeostasis and (p)ppGpp has recently been reported in *B. subtilis* [124]. The (p)ppGpp synthetase/hydrolase, Rel, was shown to interact with DarB, a protein of unknown function exclusively constituted of a c-di-AMP binding domain. Upon K^+ limitation, interaction with this c-di-AMP binding protein resulted in a significant (p)ppGpp accumulation [124]. Interaction between Rel and DarB is inhibited by c-di-AMP. As a consequence, Rel and DarB interact exclusively in low K^+ conditions when intracellular c-di-AMP levels are low.

Detecting intracellular (p)ppGpp levels in K^+-depleted conditions could certainly verify if an accumulation of (p)ppGpp is responsible for extending the swarmer phase upon K^+ depletion. In addition, our preliminary data suggest that in *C. crescentus*, KdpD interacts with HPr rather that $EIIA^{Ntr}$ in *E. coli*. Pull-down assays performed in our lab have identified KdpD as an interactant of both forms of HPr, phosphorylated and unphosphorylated. Bacterial two-hybrid assays could further confirm this interaction *in vivo*.

Interestingly, *C. crescentus* KdpD lacks a GAF domain, which was proposed in *E. coli* to be responsible for intracellular K^+ sensing [59]. Thus, it is tempting to speculate that the GAF domain of EI^{Ntr} serves as a sensor not only for intracellular glutamine levels but also for intracellular K^+. Upon K^+ limitation, the phosphorylation of EI^{Ntr} could on one hand promote (p)ppGpp accumulation and on the other hand promote K^+ uptake through the stimulation of KdpD kinase activity via HPr interaction (Fig. 16).

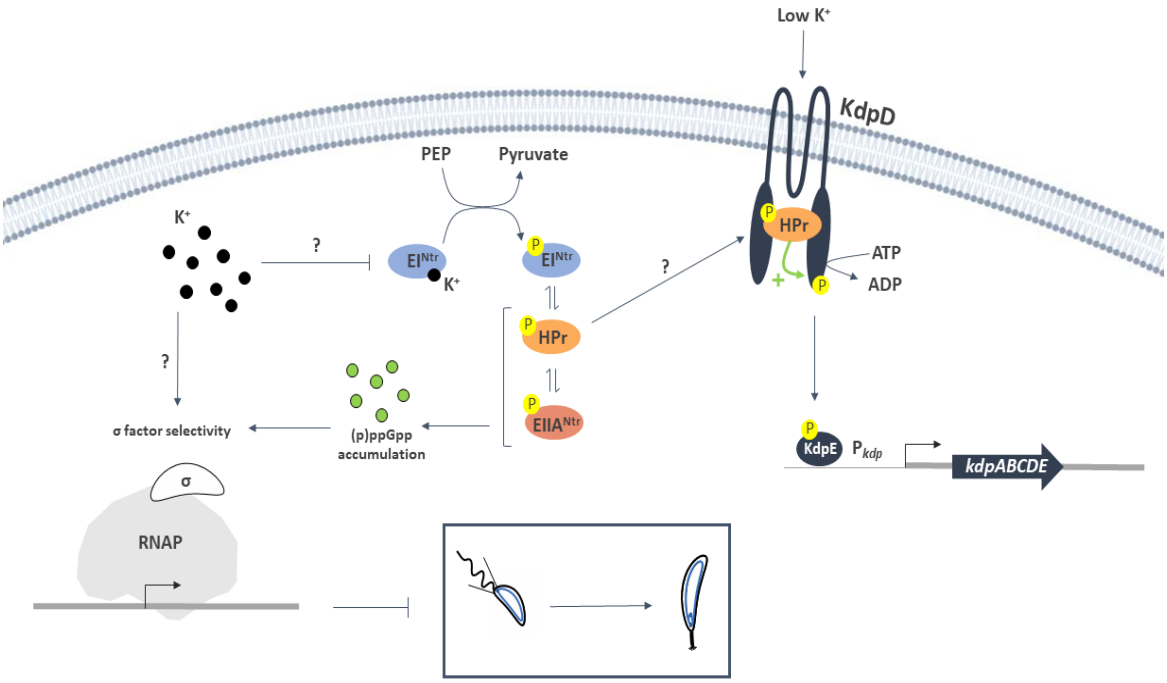

Figure 16. Working model of K^+ homeostasis and K^+-dependent control of cell cycle in *C. crescentus.*
Reminiscently to glutamine, intracellular K^+ may bind the GAF domain of EI^{Ntr} and inhibit its phosphorylation. Upon K^+ limitation, the latter inhibition would be relieved and EI^{Ntr} would subsequently phosphorylate its PTS^{Ntr} downstream components. On one hand, this cascade would promote K^+ uptake by stimulating KdpD kinase activity through an interaction with phosphorylated HPr. On the other hand, both phosphorylated HPr and $EIIA^{Ntr}$ trigger (p)ppGpp accumulation, thereby affecting the selectivity of RNAP for sigma factors and consequently delaying cell cycle progression. Sigma factor selectivity may also be directly modulated by intracellular K^+ levels.

While regulation of K^+ homeostasis seems to be a central role for second messengers, their intracellular levels are likewise under the control of K^+. Such feedback loops add complexity to the understanding of the regulatory networks connecting second messengers and K^+.

2 Kdp-mediated K^+ transport

Our data indicate that the Kdp system primarily serves K^+ uptake in low K^+ (Fig. 11). Nonetheless, Kdp is unlikely the sole K^+-transport system involved in this context. Despite its growth defect, Δ*kdpABC* was still able to grow in low K^+. Since K^+-depletion leads to a growth arrest in *C. crescentus*, this implies that K^+ is transported within cells through additional paths to Kdp, at least in low K^+ conditions. *C. crescentus* also harbours a Kup transporter and a putative K^+ channel (CCNA_01688) that may be involved in this transport. Consequent to the importance of Kup, Tn-seq data in our lab suggest that this transporter is essential in complex and minimal media.

Whatever the way K^+ is transported in the absence of the Kdp system, it would be interesting to check whether this second transport system is under the control of KdpE and/or KdpD. Indeed, the ability Δ*kdpD* cells to grow at higher OD than wild-type cells in low K^+ conditions whereas on the contrary, Δ*kdpABC* cells poorly grew in same conditions suggests that KdpD negatively regulates this secondary K^+ transport (Fig. 12A). And since the phospho-mimetic mutant of KdpE ($kdpE_{D56E}$) behaves similarly to Δ*kdpD* while the corresponding phospho-inactive mutant $kdpE_{D56A}$ and Δ*kdpE* behave rather like Δ*kdpABC* (Fig. 12A), it is tempting to speculate that the phosphorylated form of KdpE

(KdpE~P) is required for this secondary K^+ transport to be active. But if this is true, it would imply another HK than KdpD to phosphorylate KdpE in a Δ*kdpD* background. An obvious candidate would be PhoR, which is conserved in *C. crescentus* and has been shown to cross-talk with KdpD/E system in *E. coli* [74] (See section 3.1 of introduction). Alternatively, it was shown in *E. coli* that KdpE could be phosphorylated by low molecular weight phosphodonors such as acetyl phosphate both *in vitro* and *in vivo* in the absence of a full length KdpD [125]. Likewise, the *E. coli* OmpR and the *Salmonella* PhoP response regulators are also phosphorylated by acetyl phosphate in the absence of their cognate HK [126,127]. To test this hypothesis, the phosphorylation level of KdpE could be determined in wild-type, Δ*kdpD* and Δ*kdpD*Δ*phoR* strains in low K^+ conditions. Determining the KdpE direct regulon by ChIP-seq would also indicate if (an)other K^+ transporter(s) is under the control of the KdpD/E system.

It is worth mentioning that after a few days of incubation on K_0 plates, Δ*kdpABC* easily accumulates bigger colonies suggesting the emergence of suppressor mutations. Whole-genome sequencing of these clones could uncover new regulators of K^+ homeostasis and highlight strategies set up to cope with the lack of K^+. In *B. subtilis*, the loss of the KtrAB and KimA transport systems lead to the accumulation of suppressors mutations increasing the synthesis of positively charged amino acids, shown to compensate the lack of K^+ [22]. Suppressor mutations increasing the selectivity of cation transporters for K^+ have also been reported in *B. subtilis* [51].

3 Regulation of *kdp* expression

Characterization of the *C. crescentus* KdpD/E TCS suggests its control over *kdp* expression differs from that of *E. coli*. While KdpE appears essential to the transcriptional activation of *kdp*, our data question the role of KdpD in that regulation. The increased doubling time in Δ*kdpD* and kdp_{H670N} supports that abolishment of the kinase activity slows down growth in low K^+ conditions (Fig. 10B). In contrast, later in growth, both mutants surpass the wild-type strain (Fig. 10A and 10C). We first considered that the growth of Δ*kdpD* could be associated to the temporal regulation of both kinase and phosphatase activities. HKs generally act as phosphate on their cognate response regulators in the absence of stimulation to autophosphorylate [128]. We therefore hypothesized that the growth pattern of Δ*kdpD* could reflect in a first step the abolishment of the kinase activity and in a second step, the abolishment of the phosphatase activity. The phosphorylated histidine residue in HK is required for both the kinase and phosphatase activities, likely explaining why the $kdpD_{H670N}$ mutant phenocopied Δ*kdpD*. Mutants that would specifically abolish either the kinase or the phosphatase activity of KdpD would allow to measure the involvement of each activity in the response to K^+ limitation. Substitution of the Thr677 residue was shown to specifically abolish the phosphatase activity of *E. coli* KdpD [59].

We also found that *kdp* was expressed in both Δ*kdpD* and $kdpD_{H670N}$ in contrast to Δ*kdpE* or $kdpE_{D56A}$ (Fig. 10D and 10E), indicating that KdpE is still phosphorylated in the absence of KdpD. As already mentioned, KdpE could, in the absence of KdpD, be phosphorylated by other phosphodonors (*e.g.* acetyl phosphate or PhoR). To test this possibility, the *kdp* expression should be measured in mutants in which both KdpD and KdpE are inactivated (Δ*kdpDE*, $kdpD_{H670N}$ $kdpE_{D56A}$, $kdpD_{H670N}$ Δ*kdpE* and Δ*kdpD* $kdpE_{D56A}$). Alternatively, *kdp* expression could be repressed by another RR than KdpE in a KdpD-dependent way, suggesting that KdpD could cross-talk with another RR. Assuming the cross-talk between PhoR/B and KdpD/E described in *E. coli* exists in *C. crescentus*, it could be possible that KdpD regulates phosphorylation of PhoB, which in turn modulates *kdp* expression. Upon K^+ limitation, KdpD could for example (i) phosphorylate KdpE and (ii) dephosphorylate PhoB~P, with

KdpE~P and PhoB~P antagonistically acting as activator and repressor of *kdp* expression, respectively. However, the recently characterized PhoB regulon in *C. crescentus* did not identify *kdp* as a PhoB binding target under phosphate limitation. Nevertheless, the PhoB-dependent transcriptional response might be slightly different under K^+ and phosphate limitation. We should aim to measure *kdp* expression in the absence of both RRs to test this possibility. A thorough characterization of the *kdp* regulation would undoubtedly be helpful to understand how *Caulobacter* cells deal with K^+ limitation.

References

1. Epstein, W. The Roles and Regulation of Potassium in Bacteria. *Prog. Nucleic Acid Res. Mol. Biol.* **75**, 293–320 (2003).

2. Danchin, A. & Nikel, P. I. Why Nature Chose Potassium. *J. Mol. Evol.* **87**, 271–288 (2019).

3. Auffinger, P., D'Ascenzo, L. & Ennifar, E. *Sodium and Potassium Interactions with Nucleic Acids*. (2016). doi:10.1007/978-3-319-21756-7

4. Leonarski, F., Ascenzo, L. D. & Auffinger, P. Nucleobase carbonyl groups are poor Mg 2 + inner-sphere binders but excellent monovalent ion binders — a critical PDB survey. *RNA* **25**, 173–192 (2019).

5. Fasano, O., De Vendittis, E. & Parmeggiani, A. Hydrolysis of GTP by Elongation Factor Tu Can Be Induced by Monovalent Cations in the Absence of Other Eflectors *. *J. Biol. Chem.* **257**, 3145–3150 (1982).

6. Wu, Y., Qian, X., He, Y., Moya, I. A. & Luo, Y. Crystal Structure of an ATPase-active Form of Rad51 Homolog from Methanococcus voltae. *J. Biol. Chem.* **280**, 722–728 (2005).

7. Viitanen, P. V *et al.* Chaperonin-Facilitated Refolding of Ribulosebisphosphate Carboxylase and ATP Hydrolysis by Chaperonin 60 (groEL) Are K + Dependent. *Biochemistry* **60**, 5665–5671 (1990).

8. Laughlin, L. T. & Reed, G. H. The Monovalent Cation Requirement of Rabbit Muscle Pyruvate Kinase Is Eliminated by Substitution of Lysine for Glutamate 117. *Arch. Biochem. Biophys.* **348**, 262–267 (1997).

9. Fan, Y., Gaffney, B. L. & Jones, R. A. RNA GG , UU Motif Binds K + but Not Mg 2 +. *Am. Chem. Soc.* **127**, 17588–17589 (2005).

10. Stahley, M. R., Adams, P. L., Wang, J. & Strobel, S. A. Structural Metals in the Group I Intron : A Ribozyme with a Multiple Metal Ion Core. *J. Mol. Biol.* **372**, 89–102 (2007).

11. Kumar, A. & Satpati, P. Principle of K+/ Na+ selectivity in the active site of group II intron at various stages of self-splicing pathway. *J. Mol. Graph. Model.* **84**, 1–9 (2018).

12. Dibrova, D. V, Galperin, M. Y., Koonin, E. V & Mulkidjanian, A. Y. Ancient Systems of Sodium / Potassium Homeostasis as Predecessors of Membrane Bioenergetics. *Biochemistry* **80**, 590–611 (2015).

13. Ban, N., Nissen, P., Hansen, J., Moore, P. B. & Steitz, T. A. The Complete Atomic Structure of the Large Ribosomal Subunit at 2 . 4 Å Resolution. *Science (80-.).* **289**, 905–921 (2000).

14. Valente, R. S. & Xavier, K. B. The Trk Potassium Transporter Is Required for RsmB-Mediated Activation of Virulence in the Phytopathogen Pectobacterium wasabiae. *J. Bacteriol.* **198**, 248–255 (2016).

15. Su, J., Gong, H., Lai, J., Main, A. & Lu, S. The Potassium Transporter Trk and External Potassium Modulate Salmonella enterica Protein Secretion and Virulence . *Infect. Immun.* **77**, 667–675 (2009).

16. Liu, Y. *et al.* Potassium transport of Salmonella is important for type III secretion and pathogenesis Printed in Great Britain. *Microbiology* **159**, 1705–1719 (2013).

17. Macgilvary, N. J., Kevorkian, Y. L. & Tan, S. Potassium response and homeostasis in Mycobacterium tuberculosis modulates environmental adaptation and is important for host colonization. *PLoS Pathog.* **15**, 1–23 (2019).

18. Tokuda, H., Nakamura, T. & Unemoto, T. Potassium Ion Is Required for the Generation of pH-Dependent Membrane Potential and ApH by the Marine Bacterium Vibrio alginolyticud. *Am. Chem. Soc.* **20**, 4198–4203 (1981).

19. Prindle, A. *et al.* Ion channels enable electrical communication in bacterial communities. *Nature* **527**, (2015).

20. Humphries, J. *et al.* Species-Independent Attraction to Biofilms through Electrical Signaling Article Species-Independent Attraction to Biofilms through Electrical Signaling. *Cell* **168**, 200–209 (2017).

21. Podell, S. *et al.* Seasonal fluctuations in ionic concentrations drive microbial succession in a hypersaline lake community. *ISME* **8**, 979–990 (2014).

22. Gundlach, J. *et al.* Adaptation of Bacillus subtilis to Life at Extreme Potassium Limitation. *Am. Soc. Microbiol.* **8**, 1–12 (2017).

23. Ana, D. F., Muñoz, S., Olivares, J., Soto, M. J. & Sanjuán, J. Role of potassium uptake systems in sinorhizobium meliloti osmoadaptation and symbiotic performance. *J. Bacteriol.* **191**, 2133–2143 (2009).

24. Quintero-yanes, A., Monson, R. E. & Salmond, G. P. C. Environmental potassium regulates bacterial flotation , antibiotic production and turgor pressure in Serratia through the TrkH transporter. *Environ. Microbiol.* **21**, 2499–2510 (2019).

25. Blackiston, D. J., Mclaughlin, K. A. & Levin, M. Bioelectric controls of cell proliferation: ion channels, membrane voltage and the cell cycle. *Cell Cycle* **8**, 3519–3528 (2009).

26. Sano, T. *et al.* Plant cells must pass a K + threshold to re-enter the cell cycle. *Plant J.* **50**, 401–413 (2007).

27. Ouadid-ahidouch, H. & Ahidouch, A. K + channels and cell cycle progression in tumor cells. *Front. Physiol.* **4**, 1–8 (2013).

28. DeCoursey, T. E., Chandy, G. K., Gupta, S. & Cahalan, M. D. Voltage-gated K+ channels in human T lymphocytes: a role in mitogenesis ? *Nature* **307**, 465–468 (1984).

29. Rouzaire-Dubois, B. & Dubois, J. M. A quantitative analysis of the role of K+ channels in mitogenesis of neuroblastoma cells. *Cell. Signal.* **3**, 333–339 (1991).

30. Stratford, J. P., Edwards, C. L. A., Ghanshyam, M. J., Malyshev, D. & Delise, M. A. Electrically induced bacterial membrane-potential dynamics correspond to cellular proliferation capacity. *PNAS* **116**, 9552–9557 (2019).

31. Urrego, D. *et al.* Potassium channels in cell cycle and cell proliferation. *Phil. Trans. R. Soc. B* **369**, 1–9 (2014).

32. Beagle, S. D. & Lockless, S. W. Unappreciated Roles for K + Channels in Bacterial Physiology. *Trends Microbiol.* **xx**, 1–9 (2020).

33. Humeau, J., Manuel, J., Pedro, B., Vitale, I. & Nu, L. Cell Calcium Calcium signaling and cell cycle : Progression or death. *Cell Calcium* **70**, 3–15 (2018).

34. Serrano-novillo, C. *et al.* Implication of Voltage-Gated Potassium Channels in Neoplastic Cell Proliferation. *Cancers (Basel).* **11**, 1–17 (2019).

35. Kuo, M. M., Haynes, W. J., Loukin, S. H., Kung, C. & Saimi, Y. Prokaryotic K + channels : From crystal structures to diversity. *FEMS Microbiol. Rev.* **29**, 961–985 (2005).

36. Vieira-pires, R. S., Szollosi, A. & Cabral, J. H. M. The structure of the KtrAB potassium transporter. *Nature* **496**, 323–329 (2013).

37. Cao, Y. *et al.* Crystal structure of a potassium ion transporter, TrkH. *Nature* **471**, 336–341 (2011).

38. Cao, Y. *et al.* Gating of the TrkH ion channel by its associated RCK protein TrkA. *Nature* **496**, 317–322 (2013).

39. Levin, E. J. & Zhou, M. Recent progress on the structure and function of the TrkH/KtrB ion channel. *Current Opinion in Structural Biology* **27**, 95–101 (2014).

40. Zhang, H. *et al.* TrkA undergoes a tetramer-to-dimer conversion to open TrkH which enables changes in membrane potential. *Nat. Commun.* **11**, (2020).

41. Gründling, A. Potassium Uptake Systems in Staphylococcus aureus : New Stories about Ancient Systems. *MBio* **4**, (2013).

42. Rhoads, D. B., Waters, F. B. & Epstein, W. Cation Transport in Escherichia coli VIII . Potassium Transport Mutants. *J. Gen. Physiol.* **67**, 325–341 (1976).

43. Holtmann, G., Bakker, E. P., Uozumi, N. & Bremer, E. KtrAB and KtrCD : Two K+ Uptake Systems in Bacillus subtilis and Their Role in Adaptation to Hypertonicity. *J. Bacteriol.* **185**, 1289–1298 (2003).

44. Kim, H. *et al.* Structural Studies of Potassium Transport Protein KtrA Regulator of Conductance of K+ (RCK) C Domain in Complex with Cyclic Diadenosine Monophosphate (c-di-AMP) *. *J. Biol. Chem.* **290**, 16393–16402 (2015).

45. Nakamura, T., Yuda, R., Unemoto, T. & Bakker, E. P. KtrAB , a New Type of Bacterial K+ - Uptake System from Vibrio alginolyticus. *J. Bacteriol.* **180**, 3491–3494 (1998).

46. Sato, Y. *et al.* Defining membrane spanning domains and crucial membrane-localized acidic amino acid residues for K þ transport of a Kup / HAK / KT-type Escherichia coli potassium transporter. *J. Biochem.* **155**, 315–323 (2014).

47. Tascón, I. *et al.* Structural basis of proton-coupled potassium transport in the KUP family. *Nat. Commun.* **11**, 1–10 (2020).

48. Quintina, I. M., Gibhardt, J., Turdiev, A. & Hammer, E. The KupA and KupB Proteins of Lactococcus lactis IL1403 Are Novel c-di-AMP Receptor Proteins Responsible for Potassium Uptake. *J. Bacteriol.* **201**, 1–13 (2019).

49. Bossemeyer, D., Schlosser, A. & Bakker, E. P. Specific cesium transport via the Escherichia coli Kup (TrkD) K+ uptake system. *J. Bacteriol.* **171**, 2219–2221 (1989).

50. Zakharyan, E. & Trchounian, A. K+ influx by Kup in Escherichia coli is accompanied by a decrease in H+ efflux. *FEMS Microbiol. Lett.* **204**, 61–64 (2001).

51. Gundlach, J. *et al.* Control of potassium homeostasis is an essential function of the second messenger cyclic di-AMP in Bacillus subtilis. *Sci. Signal.* **10**, 1–10 (2017).

52. Huang, C., Pedersen, B. P. & Stokes, D. L. Crystal structure of the potassium-importing KdpFABC membrane complex. *Nature* **546**, 681–685 (2017).

53. Pedersen, B. P., Stokes, D. L. & Apell, H. The KdpFABC complex – K+ transport against all odds.

Mol. Membr. Biol. **35**, 21–38 (2019).

54. Irzik, K., Pfro, J., Goss, T., Ahnert, F. & Haupt, M. The KdpC subunit of the Escherichia coli K + -transporting KdpB P-type ATPase acts as a catalytic chaperone. *FEBS J.* **278**, 3041–3053 (2011).

55. Greie, J. The KdpFABC complex from Escherichia coli : A chimeric K + transporter merging ion pumps with ion channels. *Eur. J. Cell Biol.* **90**, 705–710 (2011).

56. Ali, M. K. *et al.* Regulation of Inducible Potassium Transporter KdpFABC by the KdpD / KdpE Two-Component System in Mycobacterium smegmatis. *Front. Microbiol.* **8**, (2017).

57. Dani, P., Ujaoney, A. K., Apte, S. K. & Basu, B. Regulation of potassium dependent ATPase (kdp) operon of Deinococcus radiodurans. *PLoS One* 1–16 (2017).

58. Xie, M., Wu, M. & Han, A. Structural insights into the signal transduction mechanism of the K + -sensing two-component system KdpDE. *Sci. Signal.* **13**, 1–12 (2020).

59. Schramke, H. *et al.* A Dual-Sensing Receptor Confers Robust Cellular Article A Dual-Sensing Receptor Confers Robust Cellular Homeostasis. *CellReports* **16**, 213–221 (2016).

60. Toro-Roman, A., Wu, T. & Stock, A. M. A common dimerization interface in bacterial response regulators KdpE and TorR. *Protein Sci.* **14**, 3077–3088 (2005).

61. Heermann, R. & Jung, K. The complexity of the 'simple' two-component system KdpD/KdpE in Escherichiacoli in Escherichia coli. *FEMS* **304**, 97–106 (2010).

62. Sweet, M. E. *et al.* Serine phosphorylation regulates the P-type potassium pump KdpFABC. *Elife* **9**, 1–19 (2020).

63. Epstein, W. The KdpD Sensor Kinase of Escherichia coli Responds to Several Distinct Signals To Turn on Expression of the Kdp Transport System. *J. Bacteriol.* **198**, 212–220 (2016).

64. Asha, H. & Gowrishankar, J. Regulation of kdp Operon Expression in Escherichia coli : Evidence against Turgor as Signal for Transcriptional Control. *J. Bacteriol.* **175**, 4528–4537 (1993).

65. Hamann, K., Zimmann, P. & Altendorf, K. Reduction of Turgor Is Not the Stimulus for the Sensor Kinase KdpD of Escherichia coli. *J. Bacteriol.* **190**, 2360–2367 (2008).

66. Laermann, V., Emina, C., Kipschull, K., Zimmann, P. & Altendorf, K. The sensor kinase KdpD of Escherichia coli senses external K +. *Mol. Microbiol.* **88**, 1194–1204 (2013).

67. Rothenbucher, M. C., Facey, S. J., Kiefer, D., Kossmann, M. & Kuhn, A. The cytoplasmic C-terminal domain of the Escherichia coli KdpD protein functions as a K+ sensor. *J. Bacteriol.* **188**, 1950–1958 (2006).

68. Heikaus, C. C., Pandit, J. & Klevit, R. E. Cyclic Nucleotide Binding GAF Domains from Phosphodiesterases – Structural and Mechanistic Insights. *Structure* **17**, 1551–1557 (2009).

69. Cann, M. A subset of GAF domains are evolutionarily conserved sodium sensors. *Mol. Microbiol.* **64**, 461–472 (2007).

70. Loukin, S. H., Kuo, M. M., Zhou, X., Haynes, W. J. & Kung, C. Microbial K+ Channels. *J. Gen. Physiol.* **125**, 521–527 (2005).

71. Miller, S., Ness, L. S., Wood, C. M., Fox, B. C. & Booth, I. R. Identification of an Ancillary Protein , YabF , Required for Activity of the KefC Glutathione-Gated Potassium Efflux System in Escherichia coli. *J. Bacteriol.* **182**, 6536–6540 (2000).

72. Healy, J. *et al.* Understanding the Structural Requirements for Activators of the Kef Bacterial Potassium Efflux System. *Biochemistry* **53**, 1982–1992 (2014).

73. Ferguson, G. P., Mclaggan, D. & Booth, R. Potassium channel activation by glutathione-S-conjugates in Escherichia coil : protection against methylglyoxal is mediated by cytoplasmic acidification. *Mol. Microbiol.* **17**, 1025–1033 (1995).

74. Schramke, H. *et al.* Revisiting regulation of potassium homeostasis in Escherichia coli : the connection to phosphate limitation. *Microbiologyopen* **6**, 1–16 (2017).

75. Weiden, P. L., Epstein, W. & Schultz, S. G. Cation Transport in Escherichia coli VII . Potassium requirement for phosphate uptake. *J. Gen. Physiol.* **50**, 1641–1661 (1967).

76. Lüttmann, D. *et al.* Stimulation of the potassium sensor KdpD kinase activity by interaction with the phosphotransferase protein IIA Ntr in Escherichia coli. *Mol. Microbiol.* **72**, 978–994 (2009).

77. Lee, C. *et al.* Potassium mediates Escherichia coli enzyme IIA Ntr -dependent regulation of sigma factor selectivity. *Mol. Microbiol.* **78**, 1468–1483 (2010).

78. Pflüger-Grau, K. & Görke, B. Regulatory roles of the bacterial nitrogen-related phosphotransferase system. *Trends Microbiol.* **18**, 205–214 (2010).

79. Lee, C., Cho, S., Yoon, M., Peterkofsky, A. & Seok, Y. Escherichia coli enzyme IIA Ntr regulates the K+ transporter TrkA. *PNAS* **104**, 4124–4129 (2007).

80. Lüttmann, D., Göpel, Y. & Görke, B. The phosphotransferase protein EIIA Ntr modulates the phosphate starvation response through interaction with histidine kinase PhoR in Escherichia coli. *Mol. Microbiol.* **86**, 96–110 (2012).

81. Moscoso, J. A. *et al.* Binding of Cyclic Di-AMP to the Staphylococcus aureus Sensor Kinase KdpD Occurs via the Universal Stress Protein Domain and Downregulates the Expression of the Kdp Potassium Transporter. *J. Bacteriol.* **198**, 98–110 (2016).

82. Gundlach, J. *et al.* Sustained sensing in potassium homeostasis : Cyclic di-AMP controls potassium uptake by KimA at the levels of. *J. Biol. Chem.* **294**, 9605–9614 (2019).

83. Gibhardt, J. *et al.* c-di-AMP assists osmoadaptation by regulating the Listeria monocytogenes potassium transporters KimA and KtrCD. *J. Biol. Chem.* (2019). doi:10.1074/jbc.RA119.010046

84. Wang, X. *et al.* A c-di-AMP riboswitch controlling kdpFABC operon transcription regulates the potassium transporter system in Bacillus thuringiensis. *Commun. Biol.* **2**, (2019).

85. Corrigan, R. M. *et al.* Systematic identi fi cation of conserved bacterial c-di-AMP receptor proteins. *PNAS* **110**, 9084–9089 (2013).

86. Nelson, J. W. *et al.* Riboswitches in eubacteria sense the second messenger c-di-AMP. *Nat. Chem. Biol.* **9**, 834–839 (2013).

87. Turnbough, C. L. J. Regulation of Bacterial Gene Expression by Transcription Attenuation. *Microbiol. Mol. Biol. Rev.* **83**, 1–25 (2019).

88. Skerker, J. M. & Laub, M. T. Cell-cycle progression and the generation of asymmetry in Caulobacter crescentus. *Nat. Rev. Microbiol.* **2**, 325–337 (2004).

89. Ronneau, S., Petit, K., De Bolle, X. & Hallez, R. Phosphotransferase-dependent accumulation of (p)ppGpp in response to glutamine deprivation in Caulobacter crescentus. *Nat. Commun.* 1–12 (2016). doi:10.1038/ncomms11423

90. Britos, L. *et al.* Regulatory Response to Carbon Starvation in Caulobacter crescentus. *PLoS One* **6**, (2011).

91. Hartl, J. *et al.* Untargeted metabolomics links glutathione to bacterial cell cycle progression. *Nat. Metab.* **2**, 153–166 (2020).

92. Lubin, E. A., Henry, J. T., Fiebig, A., Crosson, S. & Laub, M. T. Identification of the PhoB regulon and role of PhoU in the phosphate starvation response of Caulobacter crescentus. *J. Bacteriol.* **198**, 187–200 (2016).

93. Dalebroux, Z. D. & Swanson, M. S. ppGpp: magic beyond RNA polymerase. *Nat. Rev. Microbiol.* **10**, 203–212 (2012).

94. Skerker, J. M. & Shapiro, L. Identification and cell cycle control of a novel pilus system in Caulobacter crescentus. *EMBO J.* **19**, 3223–3234 (2000).

95. Casadaban, M. J. & Cohen, S. N. Analysis of gene control signals by DNA fusion and cloning in Escherichia coli. *J. Mol. Biol.* **138**, 179–207 (1980).

96. Evinger, M. & Agabian, N. Envelope associated nucleoid from Caulobacter crescentus stalked and swarmer cells. *J. Bacteriol.* **132**, 294–301 (1977).

97. Miller, J. H. *Experiments in Molecular Genetics*. (1972). doi:10.1006/bbrc.2001.6152

98. Pini, F. *et al.* Cell Cycle Control by the Master Regulator CtrA in Sinorhizobium meliloti. *PLoS Genet.* **11**, 1–24 (2015).

99. Li, H. & Durbin, R. Fast and accurate short read alignment with Burrows-Wheeler transform. **25**, 1754–1760 (2009).

100. Li, H. *et al.* The Sequence Alignment/Map format and SAMtools. *Bioinforma. Appl. NOTE* **25**, 2078–2079 (2009).

101. Zhang, Y. *et al.* Model-based analysis of ChIP-Seq (MACS). *Genome Biol.* **9**, (2008).

102. Rost, B. Twilight zone of protein sequence alignments. *Protein Eng.* **12**, 85–94 (1999).

103. Kumar, S., Gillilan, R. E. & Yernool, D. A. Structure and function of the juxtamembrane GAF domain of potassium biosensor KdpD. *Protein Sci.* **29**, 2009–2021 (2020).

104. Rhoads, D. B., Woo, A. & Epstein, W. Discrimination between Rb+ and K+ by Escherichia coli. *Biochim. Biophys. Acta* **469**, 45–51 (1977).

105. Gorbatyuk, B. & Marczynski, G. T. Regulated degradation of chromosome replication proteins DnaA and CtrA in Caulobacter crescentus. *Mol. Microbiol.* **55**, 1233–1245 (2005).

106. England, J. C., Perchuk, B. S., Laub, M. T. & Gober, J. W. Global regulation of gene expression and cell differentiation in Caulobacter crescentus in response to nutrient availability. *J. Bacteriol.* **192**, 819–833 (2010).

107. Gohara, D. W. & Di Cera, E. Molecular mechanisms of enzyme activation by monovalent cations. *J. Biol. Chem.* **291**, 20840–20848 (2016).

108. Klenow, H. & Henningsen, I. Effect of Monovalent Cations on the Activity of the DNA Polymerase of Escherichia coli B. *Eur. J. Biochem.* **9**, 133–141 (1969).

109. Gubaev, A. & Klostermeier, D. Potassium ions are required for nucleotide-induced closure of gyrase N-gate. *J. Biol. Chem.* **287**, 10916–10921 (2012).

110. Liu, L. F. & Wang, J. C. *Micrococcus luteus DNA gyrase: Active components and a model for its*

supercoiling of DNA (positive superhelical DNA/DNA topoisomerase). **75**, (1978).

111. Dalvie, E. D. & Osheroff, N. DNA Topoisomerases: Type II. in *Reference Module in Life Sciences* (Elsevier, 2020). doi:10.1016/b978-0-12-809633-8.21378-2

112. Sissi, C. *et al.* The effects of metal ions on the structure and stability of the DNA gyrase B protein. *J. Mol. Biol.* **353**, 1152–1160 (2005).

113. Ahijado-Guzmán, R. *et al.* Control by potassium of the size distribution of escherichia coli FtsZ polymers is independent of GTPase activity. *J. Biol. Chem.* **288**, 27358–27365 (2013).

114. Tadros, M., González, J. M., Rivas, G., Vicente, M. & Mingorance, J. Activation of the Escherichia coli cell division protein FtsZ by a low-affinity interaction with monovalent cations. *FEBS Lett.* **580**, 4941–4946 (2006).

115. Strahl, H. & Hamoen, L. W. Membrane potential is important for bacterial cell division. *Proc. Natl. Acad. Sci. U. S. A.* **107**, 12281–12286 (2010).

116. Novo, D., Perlmutter, N. G., Hunt, R. H. & Shapiro, H. M. Accurate flow cytometric membrane potential measurement in bacteria using diethyloxacarbocyanine and a ratiometric technique. *Cytometry* **35**, 55–63 (1999).

117. Biondi, E. G. *et al.* A phosphorelay system controls stalk biogenesis during cell cycle progression in Caulobacter crescentus. *Mol. Microbiol.* **59**, 386–401 (2006).

118. Brun, Y. V. & Shapiro, L. A temporally controlled σ-factor is required for polar morphogenesis and normal cell division in Caulobacter. *Genes Dev.* **6**, 2395–2408 (1992).

119. Christen, M. *et al.* DgrA is a member of a new family of cyclic diguanosine monophosphate receptors and controls flagellar motor function in Caulobacter crescentus. *PNAS* **104**, 4112–4117 (2007).

120. Gonzalez, D. & Collier, J. Effects of (p)ppGpp on the progression of the cell cycle of caulobacter crescentus. *J. Bacteriol.* **196**, 2514–2525 (2014).

121. Wang, J. D., Sanders, G. M. & Grossman, A. D. Nutritional Control of Elongation of DNA Replication by (p)ppGpp. *Cell* **128**, 865–875 (2007).

122. Jishage, M., Kvint, K., Shingler, V. & Nyström, T. Regulation of σ factor competition by the alarmone ppGpp. *GENES Dev.* **70**, 1260–1270 (2002).

123. Sharma, R., Shimada, T., Mishra, V. K., Upreti, S. & Sardesai, A. A. Growth inhibition by external potassium of Escherichia coli lacking PtsN (EIIANtr) is caused by potassium limitation mediated by YcgO. *J. Bacteriol.* **198**, 1868–1882 (2016).

124. Krüger, L. *et al.* A rendezvous of two second messengers: The c-di-AMP receptor protein DarB controls (p)ppGpp synthesis in Bacillus subtilis. *unpuplished* (2020).

125. Heermann, R., Altendorf, K. & Jung, K. The N-terminal Input Domain of the Sensor Kinase KdpD of Escherichia coli Stabilizes the Interaction between the Cognate Response Regulator KdpE and the Corresponding DNA-binding Site. *J. Biol. Chem.* **278**, 51277–51284 (2003).

126. Matsubara, M. & Mizuno, T. EnvZ-independent phosphotransfer signaling pathway of the ompr-mediated osmoregulatory expression of ompc and ompf in escherichi. *Bioscience, Biotechnology and Biochemistry* **63**, 408–414 (1999).

127. Chamnongpol, S. & Groisman, E. A. Acetyl phosphate-dependent activation of a mutant PhoP response regulator that functions independently of its cognate sensor kinase. *J. Mol. Biol.* **300**, 291–305 (2000).

128. Capra, E. J. & Laub, M. T. The Evolution of Two-Component. *Annu Rev Microbiol.* **66**, 325–347 (2012).

Supplementary figures

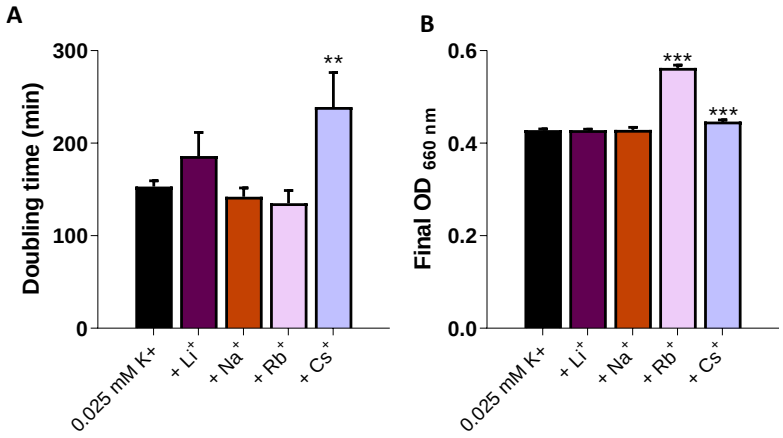

Figure 1. Supplementation of low K^+ conditions with Li^+, Na^+, Rb^+ and Cs^+. Alkali metals were added at a concentration of 0.5 mM. Doubling times (A) and final ODs (B). Statistical analyses were carried out via one-way ANOVA followed by Tukey's test for multiple comparisons. Error bars= ±SD; n=3.

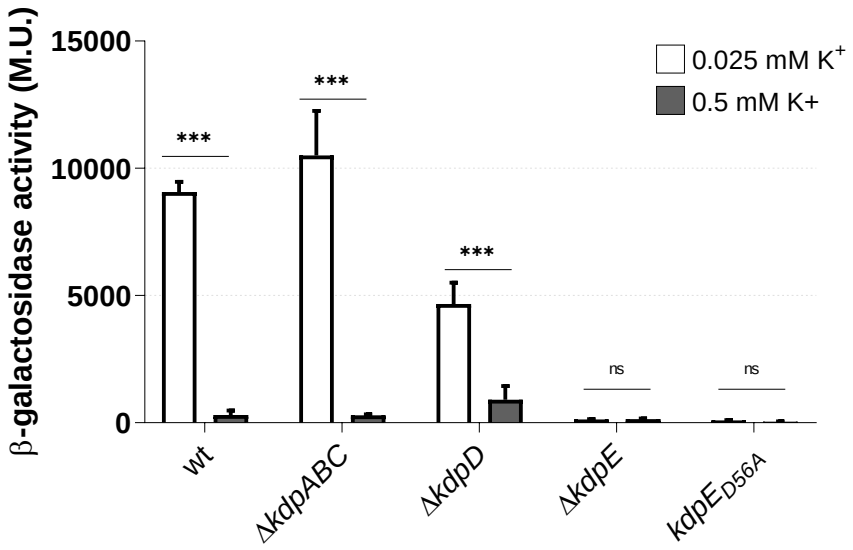

Figure 2. Substitution the catalytic aspartate in KdpE (*kdpE*$_{D56A}$) abolishes *kdp* expression.
β-Galactosidase activities of a *kdp*$_{D56A}$ strain carrying a transcriptional P$_{kdp}$::*lacZ* fusion grown in low and high K^+ compared with other strains presented in Fig. 12D. Data on *kdpE*$_{D56A}$ strain was not collected simultaneously with wild-type, Δ*kdpABC*, Δ*kdpD* and Δ*kdpE* strains. Statistical analyses were carried out via two-ways ANOVA followed by Tukey's test for multiple comparisons. Error bars= ±SD; n=3.

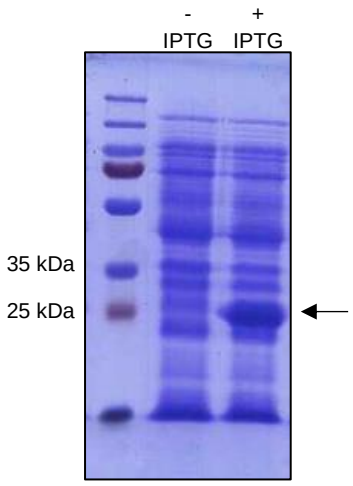

Figure 3. Expression of KdpE upon IPTG induction (arrow) in *E. coli* BL21 (DE3) pLysS strain harbouring plasmid pET-28a-*kdpE*.